

See discussions, stats, and author profiles for this publication at: <https://www.researchgate.net/publication/344944690>

Hogwild! over Distributed Local Data Sets with Linearly Increasing Mini-Batch Sizes

Preprint · October 2020

CITATIONS

0

READS

23

6 authors, including:



Marten van Dijk
RSA Laboratories

151 PUBLICATIONS 6,777 CITATIONS

SEE PROFILE



Nhuong Nguyen
University of Connecticut

6 PUBLICATIONS 0 CITATIONS

SEE PROFILE



Toan Nguyen
University of Connecticut

4 PUBLICATIONS 0 CITATIONS

SEE PROFILE



Lam M. Nguyen
IBM Research

52 PUBLICATIONS 393 CITATIONS

SEE PROFILE

Some of the authors of this publication are also working on these related projects:



Efficient methods for self-concordant optimization [View project](#)



Supply Chain Management [View project](#)

HOGWILD! OVER DISTRIBUTED LOCAL DATA SETS WITH LINEARLY INCREASING MINI-BATCH SIZES

Marten van Dijk^{1,2*}, Nhung V. Nguyen^{3†*}, Toan N. Nguyen^{3†},
Lam M. Nguyen⁴, Quoc Tran-Dinh⁵, Phuong Ha Nguyen⁶

¹ CWI Amsterdam, The Netherlands

² Department of Electrical and Computer Engineering, University of Connecticut, CT, USA

³ Department of Computer Science and Engineering, University of Connecticut, CT, USA

⁴ IBM Research, Thomas J. Watson Research Center, Yorktown Heights, NY, USA

⁵ Department of Statistics and Operations Research,
The University of North Carolina at Chapel Hill, Chapel Hill, NC, USA,

⁶ eBay, CA, USA

marten.van.dijk@cwi.nl, nhung.nguyen@uconn.edu, nntoan2211@gmail.com,
LamNguyen.MLTD@ibm.com, quoctd@email.unc.edu, phuongha.ntu@gmail.com

ABSTRACT

Hogwild! implements asynchronous Stochastic Gradient Descent (SGD) where multiple threads in parallel access a common repository containing training data, perform SGD iterations, and update shared state that represents a jointly learned (global) model. We consider big data analysis where training data is distributed among local data sets in a heterogeneous way – and we wish to move SGD computations to local compute nodes where local data resides. The results of these local SGD computations are aggregated by a central “aggregator” which mimics Hogwild!. We show how local compute nodes can start choosing small mini-batch sizes which increase to larger ones in order to reduce communication cost (round interaction with the aggregator). We improve state-of-the-art literature and show $O(\sqrt{K})$ communication rounds for heterogeneous data for strongly convex problems, where K is the total number of gradient computations across all local compute nodes. For our scheme, we prove a *tight* and novel non-trivial convergence analysis for strongly convex problems for *heterogeneous* data which does not use the bounded gradient assumption as seen in many existing publications. The tightness is a consequence of our proofs for lower and upper bounds of the convergence rate, which show a constant factor difference. We show experimental results for plain convex and non-convex problems for biased (i.e., heterogeneous) and unbiased local data sets.

1 Introduction

The optimization problem for training many Machine Learning (ML) models using a training set $\{\xi_i\}_{i=1}^M$ of M samples can be formulated as a finite-sum minimization problem as follows

$$\min_{w \in \mathbb{R}^d} \left\{ F(w) = \frac{1}{M} \sum_{i=1}^M f(w; \xi_i) \right\}.$$

The objective is to minimize a loss function with respect to model parameters w . This problem is known as empirical risk minimization and it covers a wide range of convex and non-convex problems from the ML domain, including, but not limited to, logistic regression, multi-kernel learning, conditional random fields and neural networks. In this paper, we are interested in solving the following more general stochastic optimization problem with respect to some

* these authors contributed equally.

† supported by NSF grant CNS-1413996 “MACS: A Modular Approach to Cloud Security.”

distribution \mathcal{D} :

$$\min_{w \in \mathbb{R}^d} \{F(w) = \mathbb{E}_{\xi \sim \mathcal{D}}[f(w; \xi)]\}, \quad (1)$$

where F has a Lipschitz continuous gradient and f is bounded from below for every ξ .

Big data analysis in the form of ML over a large training set distributed over local databases requires computation to be moved to compute nodes where local training data resides. Local SGD computations are communicated to a central ‘‘aggregator’’ who maintains a global model. Local computations are executed in parallel and resulting SGD updates arrive out-of-order at the aggregator. For this purpose we need robust (in terms of convergence) asynchronous SGD.

Our approach is based on the Hogwild! [Recht et al., 2011] recursion

$$w_{t+1} = w_t - \eta_t \nabla f(\hat{w}_t; \xi_t), \quad (2)$$

where \hat{w}_t represents the vector used in computing the gradient $\nabla f(\hat{w}_t; \xi_t)$ and whose vector entries have been read (one by one) from an aggregate of a mix of previous updates that led to w_j , $j \leq t$. In a single-thread setting where updates are done in a fully consistent way, i.e. $\hat{w}_t = w_t$, yields SGD with diminishing step sizes $\{\eta_t\}$.

Recursion (2) models asynchronous SGD. We define the amount of asynchronous behavior by function $\tau(t)$:

Definition 1. We say that the sequence $\{w_t\}$ is consistent with a delay function τ if, for all t , vector \hat{w}_t includes the aggregate of the updates up to and including those made during the $(t - \tau(t))$ -th iteration*, i.e., $\hat{w}_t = w_0 - \sum_{j \in \mathcal{U}} \eta_j \nabla f(\hat{w}_j; \xi_j)$ for some \mathcal{U} with $\{0, 1, \dots, t - \tau(t) - 1\} \subseteq \mathcal{U}$.

Our main insight is that the asynchronous SGD framework based on Hogwild! can resist much larger delays than the natural delays caused by the network communication infrastructure, in fact, it turns out that $\tau(t)$ can scale as much as $\approx \sqrt{t/\ln t}$ for strongly convex problems [Nguyen et al., 2018, 2019a]. This means that recurrence (2) can be used/exploited in an asynchronous SGD implementation over distributed local data sets where much more *asynchronous behavior is introduced by design*.

In our setting where SGD recursions are executed locally at compute nodes where biased (i.e., heterogeneous) local training data resides, compute nodes execute SGD recursions in ‘rounds’. From the perspective of a local compute node, a round consists of the sequence of SGD recursions between two consecutive ‘update’ communications to the central aggregator. Within a round, w_t is iteratively updated by subtracting $\eta_t \nabla f(\hat{w}_t; \xi_t)$. The sum of updates $\sum_{t \in \text{round}} \eta_t \nabla f(\hat{w}_t; \xi_t)$ is communicated to the aggregator at the end of the round after which a new round starts leading to a next sum of updates to be communicated at the end of the next round. Locally, compute nodes receive (out of sync) broadcast messages with the current global model from the central aggregator (according to some strategy, e.g., on average one or two such messages per round). This is used to replace their local model w_t computed so far. Details are given in Section 3.

Rather than having each round execute the same/constant number of SGD recursions, this paper builds on our main observation that we are allowed to introduce asynchronous behavior by design while still maintaining convergence (as we will see at a rate that matches a *lower bound* up to a constant). We propose to *increase the number of SGD iterations performed locally at each compute node from round to round*. This *reduces the amount of network communication* compared to the straightforward usage of recurrence (2) where each compute node performs a fixed number of SGD iterations within each round.

In the distributed data setting, each local compute node may only execute for a fraction of an epoch (where the number of iterations, i.e., gradient computations, in an epoch is equal to the size of the global big training data set defined as the collection of all local training data sets together). In order to disperse to all local compute nodes information from local updates by means of updating the global model and receiving feedback from the global model (maintained at the central aggregator), there needs to be a sufficient number of round interactions. For the best convergence, we need to have more round interactions at the very start where local updates contain the most (directional) information about (where to find) the global minimum to which we wish to converge. This corresponds to small ‘sample’ sizes (measured in the number of local SGD updates within a round) in the beginning. And in order to gain as much useful information about where to find the global minimum, initial local updates should use larger step sizes (learning rate).

From our theory we see that in order to bootstrap convergence it is indeed the best to start with larger step sizes and start with rounds of small sample size after which these rounds should start increasing in sample size and should start using smaller and smaller step sizes for best performance (in terms of minimizing communication while still achieving high test accuracy). Experiments confirm our expectations.

* (2) defines the $(t + 1)$ -th iteration, where $\eta_t \nabla f(\hat{w}_t; \xi_t)$ represents the $(t + 1)$ -th update.

Contributions. For the distributed data setting where SGD recursions are executed locally at compute nodes where local training data resides and which update a global model maintained at a centralized aggregator, we introduce a new SGD algorithm based on Hogwild! [Recht et al., 2011] which does not use fixed-sized mini-batch SGD at the local compute nodes but uses increasing mini-batch (sample) sizes from round interaction to round interaction:

[I] The compute nodes and server can work together to create a global model in asynchronous fashion, where we assume that messages/packets never drop; they will be re-sent but can arrive out of order. In Theorem 1 we characterize distribution \mathcal{D} in the stochastic optimization problem (1) to which the global model relates.

[II] Given a specific (strongly convex, plain convex or non-convex) stochastic optimization problem, we may assume (believe in) a delay function τ which characterizes the maximum asynchronous behavior which our algorithm can resist for the specific problem. Given the delay function τ , we provide a general recipe for constructing increasing sample size sequences and diminishing round step size sequences so that our algorithm maintains τ as an invariant. For strongly convex problems, [Nguyen et al., 2018, 2019a] prove that $\tau(t)$ can be as large as $\approx \sqrt{t/\ln t}$ for which our recipe shows a diminishing round step size sequence of $O(\frac{\ln i}{i^2})$, where i indicates the round number, that allows a sample size sequence of $\Theta(\frac{i}{\ln i})$; the sample size sequence can almost *linearly* increase from round to round.

[III] For strongly convex problems with ‘linearly’ increasing sample size sequences $\Theta(\frac{i}{\ln i})$ we prove in Theorem 2 an upper bound of $O(1/t)$ on the expected convergence rate $\mathbb{E}[\|w_t - w_*\|^2]$, where w_* represents the global minimum in (1) and t is the SGD iteration number (each local node computes a subset of the w_t). In fact, the concrete expression of the upper bound attains for increasing t the best possible convergence rate (among stochastic first order algorithms) within a constant factor $\leq 8 \cdot 36^2$, see Corollary 1 which directly applies the lower bound from [Nguyen et al., 2019b].

[IV] Let K be the total number of gradient computations (summed over all local nodes) needed for the desired test accuracy, and let T be the number of communication rounds in our algorithm. Then, T scales less than linear with K due to the increasing sample size sequence (if a constant sample size sequence is used, i.e., fixed-sized mini-batch SGD at each of the local compute nodes, then $T = O(K)$). For strongly convex problems with diminishing step sizes we show $T = O(\sqrt{K})$ for heterogeneous local data while having $O(1/K)$ convergence rate. This implies that using diminishing step sizes give a much better performance compared to constant step sizes in terms of communication.

[V] Experiments for linearly increasing sample size sequences for strongly convex problems as well as plain convex and non-convex problems confirm the robustness of our algorithm in terms of good test accuracies (our theoretical understanding from strongly convex problems seems to generalize to plain and non-convex problems). We use biased local training data sets (meaning different compute nodes see differently biased subsets of training data) and compare to unbiased local training data sets.

2 Related Work

Unbiased Local Data (iid). For strongly convex problems with unbiased local data sets, [Stich, 2018] showed $O(1/K)$ convergence rate for $O(\sqrt{K})$ communication rounds. For the iid case this was improved by [Spiridonoff et al., 2020] to just 1 communication round, where each client performs local SGD separately after which in “one shot” all local models are aggregated (averaged) – this corresponds to $O(n)$ total communication for n clients. This result was generalized by [Khaled et al., 2020]. Based on the strong Polyak-Lojasiewicz (PL) assumption (which is a generalization of strong convexity but covers certain nonconvex models), [Yu and Jin, 2019] proved for the iid case a convergence rate of $O(1/K)$ with $\log(K/n)$ communication rounds with an exponentially increasing sample size sequence. For non-convex problems, [Yu and Jin, 2019] proved for the iid case the standard convergence rate $O(1/\sqrt{K})$ (as defined for non-convex problems) with $O(\sqrt{K} \log(K/n^2))$ communication rounds.

Biased Local Data (heterogeneous). Our focus is on heterogeneous data between different clients (this needs more communication rounds in order to achieve convergence, one-shot averaging is not enough): [Khaled et al., 2020] were the first to analyze the convergence rate for plain convex problems in this scenario. They use the bounded variance assumption in their analysis with constant step-size and with sample size sequences where sample sizes are bound by an a-priori set parameter H . They prove that $O(1/\sqrt{K})$ convergence rate (optimal for plain convex) is achieved for $O(K^{3/4})$ communication rounds (see their Corollary 5 and notice that their algorithm uses $(K/n)/H$ communication rounds). For strongly convex problems in the *heterogeneous* case (without assuming bounded variance), we show that *convergence rate $O(1/K)$ (optimal for strongly convex) is achieved for $O(\sqrt{K})$ communication rounds.*

Asynchronous Training. Asynchronous training [Zinkevich et al., 2009, Lian et al., 2015, Zheng et al., 2017, Meng et al., 2017, Stich, 2018, Shi et al., 2019] is widely used in traditional distributed SGD. Hogwild!, one of the most famous asynchronous SGD algorithms, was introduced in [Recht et al., 2011] and various variants with a fixed and

diminishing step size sequences were introduced in [Mania et al., 2015, De Sa et al., 2015, Leblond et al., 2018, Nguyen et al., 2018]. Typically, asynchronous training converges faster than synchronous training in real time due to parallelism. This is because in a synchronized solution compute nodes have to wait for the slower ones to communicate their updates after which a new global model can be downloaded by everyone. This causes high idle waiting times at compute nodes. Asynchronous training allows compute nodes to continue executing SGD recursions based on stale global models. For non-convex problems, synchronous training [Saeed Ghadimi, 2013] and asynchronous training with bounded staleness [Lian et al., 2015], or in our terminology bounded delay, achieves the same convergence rate of $O(1/\sqrt{K})$, where K is the total number of gradient computations.

The methods cited above generally use mini-batch SGD (possibly with diminishing step sizes from round to round) at each of the distributed computing threads, hence, parallelism will then lead to asynchronous behavior dictated by a delay τ which can be assumed to be bounded. Assuming bounded delays, the convergence rate is mathematically analysed in the papers cited above with the exception of [Nguyen et al., 2018, 2019a] which also analyses the convergence rate for unbounded delays (i.e., increasing delay functions τ).

As explained in this introduction, *this paper exploits the advantage of being able to resist much more asynchronous behavior than bounded delay*. We show how one can use diminishing step sizes alongside increasing sample sizes (mini-batch sizes) from round to round. This provides a technique complimentary to [Zinkevich et al., 2009, Lian et al., 2015, 2017, Zheng et al., 2017, Meng et al., 2017, Stich, 2018, Shi et al., 2019] with which current asynchronous training methods can be enhanced at the benefit of reduced communication – which is important when training over distributed local data sets in big data analysis. For example, rather than sending gradients to the server after each local update, which is not practical for edge devices (such as mobile or IoT devices) due to unreliable and slow communication, [Shi et al., 2019] introduces the idea of using a tree like communication structure which aggregates local updates in pairs from leafs to root – this technique for meeting throughput requirements at the centralized server can be added to our technique of increasing sample sizes from round to round. As another example, [Lian et al., 2017] introduces asynchronous decentralized SGD where local compute nodes do not communicate through a centralized aggregator but instead perform a consensus protocol – our technique of increasing sample sizes is complementary and can possibly be beneficial to use in this decentralized network setting. Similarly, our technique may apply to [Jie Xu, 2020], where the authors studied a new asynchronous decentralized SGD with the goal of offering privacy guarantees. We stress that our setting is asynchronous centralized SGD and is completely different from asynchronous decentralized SGD algorithms as in [Shi et al., 2019, Lian et al., 2017, Jie Xu, 2020].

Federated Learning and Local SGD. Federated Learning (FL) [Chen et al., 2016, McMahan et al., 2016] is a distributed machine learning approach which enables training on a large corpus of decentralized data located on devices like mobile phones or IoT devices. Federated learning brings the concept of “bringing the code to the data, instead of the data to the code” [Bonawitz et al., 2019]. Google [Konečný et al., 2016] demonstrated FL for the first time at a large scale when they conducted experiments of training a global model across all mobile devices via the Google Keyboard Android application [McMahan and Ramage, 2017].

Original FL requires synchrony between the server and clients (compute nodes). It requires that each client sends a full model back to the server in each round and each client needs to wait for the next computation round. For large and complicated models, this becomes a main bottleneck due to the asymmetric property of internet connection and the different computation power of devices [Chen et al., 2019a, Konečný et al., 2016, Wang et al., 2019, Hsieh et al., 2017].

In [Xie et al., 2019, Chen et al., 2019b] asynchronous training combined with federated optimization is proposed. Specifically, the server and workers (compute nodes) conduct updates asynchronously: the server immediately updates the global model whenever it receives a local model from clients. Therefore, the communication between the server and workers is non-blocking and more effective. We notice that [Xie et al., 2019] provides a convergence analysis, while [Chen et al., 2019b] does not.

In [Li et al., 2019], the authors introduce FedProx which is a modification of FedAvg (i.e., original FL algorithm of [McMahan et al., 2016]). In FedProx, the clients solve a proximal minimization problem rather than traditional minimization as in FedAvg. For theory, the authors use B -local dissimilarity and bounded dissimilarity assumptions for the global objective function. This implies that there is a bounded gradient assumption applied to the global objective function. Moreover, their proof requires the global objective function to be strongly convex.

One major shortcoming in the terms of convergence analysis of asynchronous SGD in many existing publications is that the bounded gradients and strongly convex assumptions are used together, e.g. [Lian et al., 2015, 2017, Mania et al., 2015, De Sa et al., 2015, Jie Xu, 2020, Xie et al., 2019, McMahan et al., 2016, Li et al., 2019]. However, the bounded gradient assumption is in conflict with assuming strong convexity as explained in [Nguyen et al., 2018, 2019a]. It implies that the convergence analysis should not use these two assumptions together to make the analysis complete.

Our method of increasing sample sizes together with its convergence analysis for strongly objective functions (which does not use the bounded gradient assumption) complements the related work in FL and local SGD. This paper analyses and demonstrates the promise of this new technique but does not claim a full end-to-end implementation of FL or distributed SGD with asynchronous learning.

3 Hogwild! & Increasing Sample Sizes

The next subsections explain our proposed algorithm together with how to set parameters in terms of a concrete round to round diminishing step size sequence and increasing sample size sequence.

3.1 Asynchronous SGD over Local Data Sets

Algorithm 1 ComputeNode_c – Local Model

```

1: procedure SETUP( $n$ ): Initialize increasing sample size sequences  $\{s_i\}_{i \geq 0}$  and  $\{s_{i,c} \approx p_c s_i\}_{i \geq 0}$  for each compute
   node  $c \in \{1, \dots, n\}$ , where  $p_c$  scales the importance of compute node  $c$ . Initialize diminishing round step sizes
    $\{\bar{\eta}_i\}_{i \geq 0}$ , a permissible delay function  $\tau(\cdot)$  with  $t - \tau(t)$  increasing in  $t$ , and a default global model for each compute
   node to start with.
2: end procedure
3:
4: procedure ISRRECEIVE( $\hat{v}, k$ ): This Interrupt Service Routine is called whenever a broadcast message with a new
   global model  $\hat{v}$  is received from the server. Once received, the compute node's local model  $\hat{w}$  is replaced with  $\hat{v}$ 
   from which the latest accumulated update  $\bar{\eta}_i \cdot U$  of the compute node in the ongoing round (as maintained in line
   17 below) is subtracted. (We notice that the  $k$ th broadcast message containing a global model  $\hat{v}$  from the server is
   transmitted by the server as soon as the updates up to and including rounds  $0, \dots, k - 1$  from all compute nodes
   have been received; thus  $\hat{v}$  includes all the updates up to and including round  $k - 1$ .)
5: end procedure
6:
7: procedure MAINCOMPUTENODE( $\mathcal{D}_c$ )
8:    $i = 0, \hat{w} = \hat{w}_{c,0,0}$ 
9:   while True do
10:     $h = 0, U = 0$ 
11:    while  $h < s_{i,c}$  do
12:       $t_{glob} = s_0 + \dots + s_i - (s_{i,c} - h) - 1$ 
13:       $t_{delay} = s_k + \dots + s_i - (s_{i,c} - h)$ 
14:      while  $\tau(t_{glob}) < t_{delay}$  do nothing
15:      Sample uniformly at random  $\xi$  from  $\mathcal{D}_c$ 
16:       $g = \nabla f(\hat{w}, \xi)$ 
17:       $U = U + g$ 
18:      Update model  $w = \hat{w} - \bar{\eta}_i \cdot g$ 
19:
20:      Update model  $\hat{w} = w$   $\triangleright w$  represents  $w_{c,i,h+1}$ 
21:       $h++$ 
22:    end while
23:    Send  $(i, c, U)$  to the Server.
24:     $i++$ 
25:  end while
26: end procedure

```

Compute node $c \in \{1, \dots, n\}$ updates its local model \hat{w} according to Algorithm 1. Lines 15, 16, 18, and 20 represent an SGD recursion where ξ is sampled from distribution \mathcal{D}_c , which represents c 's local data set. Variable U , see line 17, keeps track of the sum of the gradients that correspond to $s_{i,c}$ samples during c 's i -th local round. This information is send to the server in line 23, who will multiply U by the round step size $\bar{\eta}_i$ and subtract the result from the global model \hat{v} . In this way each compute node contributes updates U which are aggregated at the server. As soon as the server has aggregated each compute node's updates for their first k local rounds, the server broadcasts global model \hat{v} . As soon as c receives \hat{v} it replaces its local model \hat{w} with $\hat{v} - \bar{\eta}_i \cdot U$ (this allows the last computed gradients in U that have not yet been aggregated into the global model at the server not to go to waste).

Line 14 shows that a compute node c will wait until t_{delay} becomes smaller than $\tau(t_{glob})$. This will happen as a result of `ISRRECEIVE`(\hat{v}, k) receiving broadcast message \hat{v} together with a larger k after which the ISR computes a new (smaller) t_{delay} . Line 14 guarantees the invariant $t_{delay} \leq \tau(t_{glob})$, where τ is initialized to some "permissible" delay function which characterizes the amount of asynchronous behavior we assume the overall algorithm can tolerate (in that the algorithm has fast convergence leading to good test accuracy).

Supplemental Material A has all the detailed pseudo code with annotated invariants.

We want to label the SGD recursions computed in each of the `MAINCOMPUTENODE`(\mathcal{D}_c) applications for $c \in \{1, \dots, n\}$ to an iteration count t that corresponds to recursion (2): We want to put all SGD recursions computed by each compute node in sequential order such that it is as if we used (2) on a single machine. This will allow us to analyse whether our algorithm leads to a sequence $\{w_t\}$ which is consistent with the initialized permissible delay function τ . In order to find an ordering based on t we define in Supplemental Material B.1 a mapping ρ from the annotated labels (c, i, h) in `MAINCOMPUTENODE` to t and use this to prove the following theorem:

Theorem 1. *Our setup, compute node, and server algorithms produce a sequence $\{w_t\}$ according to recursion (2) where $\{\xi_t\}$ are selected from distribution $\mathcal{D} = \sum_{c=1}^n p_c \mathcal{D}_c$. Sequence $\{w_t\}$ is consistent with delay function τ as defined in SETUP.*

The theorem tells us that the algorithms implement recursion (2) for distribution $\mathcal{D} = \sum_{c=1}^n p_c \mathcal{D}_c$, i.e., a convex combination of each of the (possibly biased) local distributions (data sets). Scaling factors p_c represent a distribution (i.e., they sum to 1) and are used to compute local sample sizes $s_{i,c} \approx p_c s_i$, where $s_i = \sum_{c=1}^n s_{i,c}$ indicates the total number of samples in rounds i across all compute nodes.

We remark that our asynchronous distributed SGD is compatible with the more general recursion mentioned in [Nguyen et al., 2018, 2019a] and explained in Supplemental Material C.1. In this recursion each client can apply a "mask" which indicates the entries of the local model that will be considered. This allows each client to only transmit the local model entries corresponding to the mask.

3.2 Delay τ

We assume that messages/packets never drop. They will be resent but can arrive out-of-order. We are robust against this kind of asynchronous behavior: The amount of asynchronous behavior is limited by $\tau(\cdot)$; when the delay is getting too large, then the client (local compute node) enters a wait loop which terminates only when `ISRRECEIVE` receives a more recent global model \hat{v} with higher k (making t_{delay} smaller). Since $\tau(t)$ increases in t and is much larger than the delays caused by network latency and retransmission of dropped packets, asynchronous behavior due to such effects will not cause clients to get stuck in a waiting loop. We assume different clients have approximately the same speed of computation which implies that this will not cause fast clients having to wait for long bursts of time.[†]

We exploit the algorithm's resistance against delays $\tau(t)$ by using increasing sample size sequences $\{s_{i,c}\}$. Since the server only broadcasts when all clients have communicated their updates for a "round" k , increasing sample sizes implies that t_{delay} can get closer to $\tau(t_{glob})$. So, sample size sequences should not increase too much: We require the property that there exists a threshold d such that for all $i \geq d$,

$$\tau \left(\sum_{j=0}^i s_j \right) \geq 1 + \sum_{j=i-d}^i s_j. \quad (3)$$

In Supplemental Material B.2 we show that this allows us to replace condition $\tau(t_{glob}) < t_{delay}$ of the waiting loop by $i > k + d$ when $i \geq d$ while still guaranteeing $t_{delay} \leq \tau(t_{glob})$ as an invariant. In practice, since sample sizes increase, we only need to require (3) for $d = 1$ (which means we allow a local lag of one communication round) in order to resist asynchronous behavior due to network latency.

3.3 Recipe Sample Size Sequence

Given a fixed budget/number of gradient computations K which the compute nodes together need to perform, an increasing sample size sequence $\{s_i\}$ reduces the number T of communication rounds/interactions (defined by update messages coming from the compute nodes with broadcast messages from the server). Convergence to an accurate solution must be guaranteed, that is, $\{s_i\}$ has to satisfy (3) if we assume τ is indeed a permissible delay function.

[†]When entering a waiting loop, the client's operating system should context switch out and resume other computation. If a client c is an outlier with slow computation speed, then we can adjust p_c to be smaller in order to have its mini-batch/sample size $s_{i,c}$ be proportionally smaller; this will change distribution \mathcal{D} and therefore change the objective function of (1).

Supplemental Material B.3 proves how a general formula for function τ translates into an increasing sample size sequence $\{s_i\}$ that satisfies (3).

Lemma 1. *Let $g > 1$. Suppose that $\tau(x) = M_1 + (x + M_0)^{1/g}$ for some $M_1 \geq d + 2$ and $M_0 \geq ((m + 1)(g - 1)/g)^{g/(g-1)}$, where $m \geq 0$ is an integer. Then*

$$s_i = \left\lceil \frac{1}{d+1} \left(\frac{m+i+1}{d+1} \frac{g-1}{g} \right)^{1/(g-1)} \right\rceil$$

satisfies property (3).

The above lemma is a direct consequence of Supplemental Material B.3 which has a more general proof that also allows functions such as $\tau(x) = M_1 + ((x + M_0)/\ln(x + M_0))^{1/g}$ (needed for analysing the convergence of strongly convex problems with $g = 2$).

3.4 Recipe Round Step Size Sequence

As soon as we have selected an increasing sample size sequence based on τ , Supplemental Material B.4 shows how we can translate the diminishing step size sequence $\{\eta_t\}$ of recurrence (2) to a diminishing round step size sequence $\{\bar{\eta}_i\}$ that only diminishes with every mini-batch s_i from round to round. The lemma below is a direct consequence of Supplemental Material B.4 which has a slightly more general statement.

Lemma 2. *Let $0 \leq q \leq 1$ and $\{E_t\}$ a constant or increasing sequence with $E_t \geq 1$. For q and $\{E_t\}$ consider the set \mathcal{Z} of diminishing step size sequences $\{\eta_t\}$ in recurrence (2) with $\eta_t = \alpha_t/(\mu(t + E_t)^q)$ where $\{\alpha_t\}$ is some sequence of values with $\alpha_0 \leq \alpha_t \leq 3 \cdot \alpha_0$.*

We assume sample size sequence $\{s_i\}$ of Lemma 1 for $g \geq 2$. For $i \geq 0$, we define $\bar{E}_i = E_{\sum_{j=0}^i s_j}$. We define $\bar{E}_{-1} = E_0$. If $\bar{E}_i \leq 2\bar{E}_{i-1}$ for $i \geq 0$ and if $s_0 - 1 \leq E_0$, then there exists a diminishing step size sequence $\{\eta_t\}$ in set \mathcal{Z} such that

$$\eta_t = \frac{\alpha_t}{\mu(t + E_t)^q} = \frac{\alpha_0}{\mu((\sum_{j=0}^{i-1} s_j) + \bar{E}_{i-1})^q} \stackrel{\text{DEF}}{=} \bar{\eta}_i$$

for $t \in \{(\sum_{j=0}^{i-1} s_j), \dots, (\sum_{j=0}^{i-1} s_j) + s_i - 1\}$.

Notice $s_i = \Theta(i^{1/(g-1)})$ and $\bar{\eta}_i = O(i^{-q \cdot (1+1/(g-1))})$.

In Supplemental Material C.3 we discuss plain and non-convex problems. We argue in both cases to choose a diminishing step size sequence of $O(t^{-1/2})$, i.e., $q = 1/2$, and to experiment with different increasing sample size sequences $\Theta(i^{1/(g-1)})$, for $g \geq 2$, to determine into what extent the presented asynchronous SGD is robust against delays. Substituting $p = 1/(g-1) \in (0, 1]$ gives sample size sequence $\Theta(i^p)$ and round step size sequence $O(i^{-(1+p)/2})$. It turns out that $p = 1$ gives a good performance and this confirms our intuition that the results from our theory on strongly convex functions in the next section generalizes in that also plain and non-convex problems have fast convergence for linearly increasing sample size sequences.

4 Convergence Rate for Strongly Convex problems

In this section we provide a round step size sequence and a sample size sequence for strongly convex problems. We show tight upper and lower bounds. For strongly convex problems, we assume the following:

Assumption 1 (L -smooth). *$f(w; \xi)$ is L -smooth for every realization of ξ , i.e., there exists a constant $L > 0$ such that, $\forall w, w' \in \mathbb{R}^d$,*

$$\|\nabla f(w; \xi) - \nabla f(w'; \xi)\| \leq L\|w - w'\|.$$

Assumption 2. *$f(w; \xi)$ is convex for every realization of ξ , i.e., $\forall w, w' \in \mathbb{R}^d$,*

$$f(w; \xi) - f(w'; \xi) \geq \langle \nabla f(w'; \xi), (w - w') \rangle.$$

Assumption 3 (μ -strongly convex). *The objective function $F : \mathbb{R}^d \rightarrow \mathbb{R}$ is a μ -strongly convex, i.e., there exists a constant $\mu > 0$ such that $\forall w, w' \in \mathbb{R}^d$,*

$$F(w) - F(w') \geq \langle \nabla F(w'), (w - w') \rangle + \frac{\mu}{2}\|w - w'\|^2.$$

Being strongly convex implies that F has a global minimum w_* . For w_* we assume:

Assumption 4 (Finite σ). Let $N = 2\mathbb{E}[\|\nabla f(w_*; \xi)\|^2]$ where $w_* = \arg \min_w F(w)$. We require $N < \infty$.

In this section we let f be L -smooth, convex, and let the objective function $F(w) = \mathbb{E}_{\xi \sim \mathcal{D}}[f(w; \xi)]$ be μ -strongly convex with finite $N = 2\mathbb{E}[\|\nabla f(w_*; \xi)\|^2]$ where $w_* = \arg \min_w F(w)$. Notice that we do not assume the bounded gradient assumption which assumes $\mathbb{E}[\|\nabla f(w; \xi)\|^2]$ is bounded for all $w \in \mathbb{R}^d$ (not only $w = w_*$ as in Assumption 4) and is in conflict with assuming strong convexity as explained in [Nguyen et al., 2018, 2019a].

4.1 Sample Size and Round Step Size Sequences

After sequentially ordering the SGD recursions from all compute nodes we end up with a Hogwild! execution as defined by recursion (2) and we may apply the results from [Nguyen et al., 2018, 2019a] that state that $\{w_t\}$ is consistent with any delay function $\tau(t) \leq \sqrt{(t/\ln t) \cdot (1 - 1/\ln t)}$. By suitably choosing such a function τ (see Supplemental Material C.2.2 for details), application of the more general Lemma 1 from Supplemental Material B.3 gives sample size sequence

$$s_i = \left\lceil \frac{m+i+1}{16(d+1)^2} \frac{1}{\ln\left(\frac{m+i+1}{2(d+1)}\right)} \right\rceil = \Theta\left(\frac{i}{\ln i}\right).$$

For a fixed number of gradient computations K , the number T of communication rounds satisfies $K = \sum_{j=0}^T s_j$. When forgetting the $\ln i$ component, this makes T proportional to \sqrt{K} – rather than proportional to K for a constant sample size sequence. This reduction in communication rounds and overall network communication is possible because we use a diminishing step size sequence (which allows us to still prove tight upper and lower bounds on the convergence rate).

For our choice of τ , we are restricted in the more general Lemma 2 from Supplemental Material B.4 to a family \mathcal{Z} of step size functions with $a_0 = 12$ and $E_t = 2\tau(t)$. For strongly convex problems we may choose $q = 1$ which gives a step size sequence $\eta_t = \alpha_t/(\mu(t + E_t)^q)$ for which the convergence rate $\mathbb{E}[\|w_t - w_*\|^2] = O(1/t)$. This results in a $O\left(\frac{\ln i}{j^2}\right)$ round step size sequence

$$\bar{\eta}_i = \frac{12}{\mu} \cdot \frac{1}{\sum_{j=0}^{i-1} s_j + 2M_1 + \sqrt{\frac{(m+1)^2/4 + \sum_{j=0}^{i-1} s_j}{\ln((m+1)^2/4 + \sum_{j=0}^{i-1} s_j)}}},$$

where

$$M_1 = \max \left\{ d + 2, 72 \cdot \frac{L}{\mu}, \frac{1}{2} \left[\frac{m+1}{16(d+1)^2} \frac{1}{\ln\left(\frac{m+1}{2(d+1)}\right)} \right] \right\}$$

4.2 Upper Bound Convergence Rate

Based on the sequences $\{s_i\}$ and $\{\bar{\eta}_i\}$ we prove in Supplemental Material C.2.2 the following upper bound on the convergence rate for strongly convex problems:[‡]

Theorem 2. For sample size sequence $\{s_i\}$ and round step size sequence $\{\bar{\eta}_i\}$ we have expected convergence rate

$$\mathbb{E}[\|w_t - w_*\|^2] \leq \frac{4 \cdot 36^2 \cdot N}{\mu^2} \frac{1}{t} + O\left(\frac{1}{t \ln t}\right). \quad (4)$$

where t represents the total number of gradient evaluations over all compute nodes performed so far.[§]

Notice that t is equal to n times the average number of grad evaluations \bar{t} per compute node, hence, convergence rate $O(1/t) = O(1/(n\bar{t}))$ showing the expected $1/n$ dependence. We also remind the reader that $s_i = \sum_c s_{i,c}$ where $s_{i,c} \approx p_c s_i$.

We do not know whether the theory for delay functions τ for strongly convex problems gives a tight bound in terms of the maximum delay[¶] for which we can prove a tight upper bound on the convergence rate. For this reason we also experiment with the larger linear $s_i = \Theta(i)$ in the strongly convex case. (For $s_i = \Theta(i)$ we have $\bar{\eta}_i = O(i^{-2})$.)

[‡]We remark that this theorem also holds for our algorithm where the compute nodes compute mini-batch SGD for the sample set and it can be adapted for the more general recursion with masks as explained in Supplemental Material C.1 (with “ $D > 1$ ”).

[§]Mapping ρ maps annotated labels to t : $w_t = w_{\rho(c,i,h)}$.

[¶]Permissible delay functions can possibly be larger than $\sqrt{(t/\ln t) \cdot (1 - 1/\ln t)}$.

As one benchmark we compare to using a constant step size $\eta = \bar{\eta}_i$. Supplemental Material C.2.1 analyses this case and shows how to choose the constant sample size $s = s_i$ (as large as $\frac{a}{L\mu(d+1)}$ for a well defined constant a) in order to achieve the best convergence rate.

4.3 Lower Bound Convergence Rate

Applying the lower bound from [Nguyen et al., 2019b] for first order stochastic algorithms shows the following corollary, see Supplemental Material C.2.3 for a detailed discussion (also on how fast the $O((\ln t)/t)$ term disappears and how this can be influenced by using different less increasing sample size sequences).

Corollary 1. *Among first order stochastic algorithms, upper bound (4) converges for increasing t to within a constant factor $8 \cdot 36^2$ of the (theoretically) best attainable expected convergence rate, which is at least $\frac{N}{2\mu^2} \frac{1}{t} (1 - O(\frac{\ln t}{t}))$ (for each t).*

Notice that the factor is independent of any parameters like L , μ , sparsity, or dimension of the model.

The corollary shows that non-parallel (and therefore synchronous) SGD can at most achieve a factor $8 \cdot 36^2$ faster convergence rate compared to our asynchronous SGD over (heterogeneous) local data sets. It remains an open problem to investigate second (and higher) order stochastic algorithms and whether their distributed versions attain tight convergence rates when increasing sample sizes and diminishing step sizes from round to round.

5 Experiments

We summarize experimental results for strongly convex, plain convex and non-convex problems with *linear increasing sample sequences* and *biased versus unbiased local data sets*.

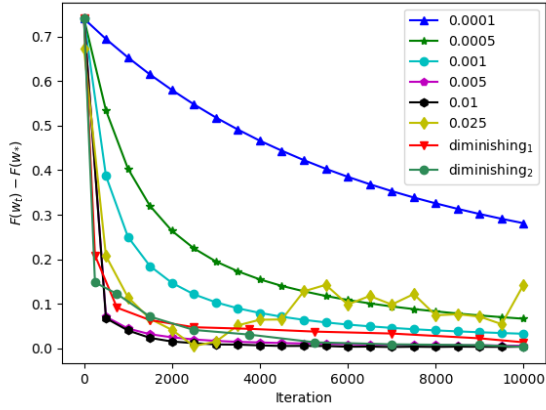
As the plain convex objective function we use logistic regression: The weight vector \bar{w} and bias value b of the logistic function can be learned by minimizing the log-likelihood function J :

$$J = - \sum_i^M [y_i \cdot \log(\sigma_i) + (1 - y_i) \cdot \log(1 - \sigma_i)],$$

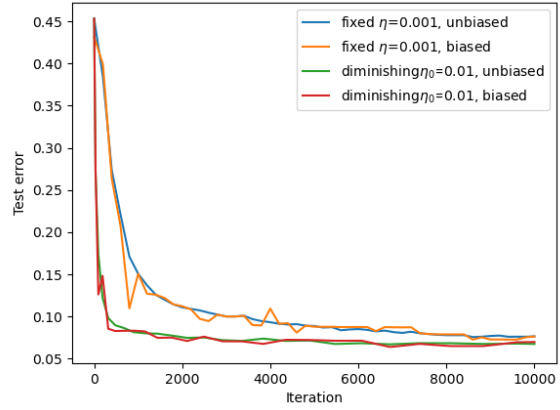
where M is the number of training samples (x_i, y_i) with $y_i \in \{0, 1\}$, and $\sigma_i = \sigma(\bar{w}, b, x_i)$ is the sigmoid function $\sigma(\bar{w}, x, b) = \frac{1}{1 + e^{-(\bar{w}^T x + b)}}$. The goal is to learn a vector w^* which represents a pair $w = (\bar{w}, b)$ that minimizes J . Function J changes into a strongly convex problem by adding ridge regularization with a regularization parameter $\lambda > 0$. i.e., we minimize $\hat{J} = J + \frac{\lambda}{2} \|w\|^2$ instead of J . For simulating non-convex problems, we choose a simple neural network (LeNet) [LeCun et al., 1998] for image classification.

We use a linearly increasing sample size sequence $s_i = a \cdot i^c + b$, where $c = 1$ and $a, b \geq 0$. For simplicity, we choose a diminishing round step size sequence corresponding to $\frac{\eta_0}{1 + \beta \cdot t}$ for the strongly convex problem and $\frac{\eta_0}{1 + \beta \cdot \sqrt{t}}$ for both the plain convex and non-convex problems, where η_0 is an initial step size. The asynchronous SGD simulation is conducted with $d = 1$, see (3).

Our asynchronous SGD with linear increasing sample sizes: Figures 1a, 2a and 3a show our proposed asynchronous SGD with linear increasing sample size sequence for constant step sizes and diminishing step sizes. We conclude that diminishing step sizes achieve (approximately) a convergence which is as fast as the convergence of the best constant step size sequence. See Supplemental Material D.2.3 for details and larger sized graphs (also for other data sets); we also show experiments in D.2.1 and D.2.2 that compare using slower increasing sample size sequences with linear sample size sequences and they all achieve approximately the same convergence rate. We conclude that using a linear sample size sequence over a constant sized one does not degrade performance – on the contrary, the number of communication rounds reduces significantly. This confirms the intuition generated by our theoretical analysis for strong convex problems which generalizes to plain and non-convex problems.

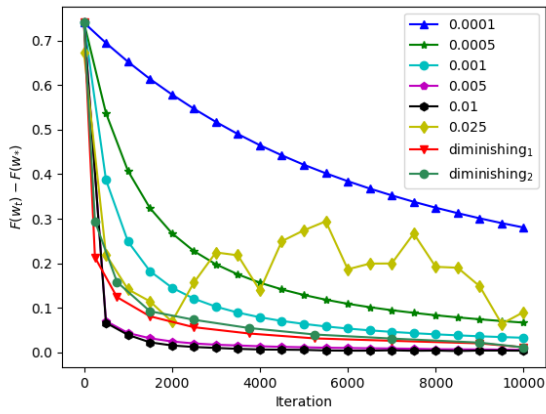


(a) Convergence rate

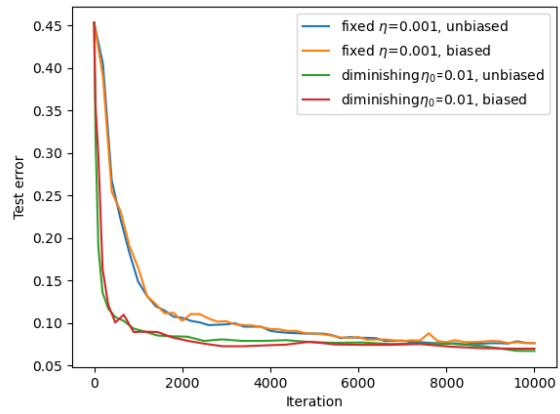


(b) Test error

Figure 1: Our asynchronous SGD for strongly convex problems: (a) The Phishing data set - various step size sequences. (b) MNIST - biased and unbiased data sets.

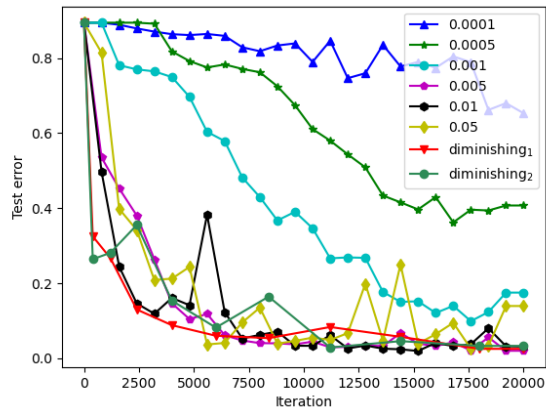


(a) Convergence rate

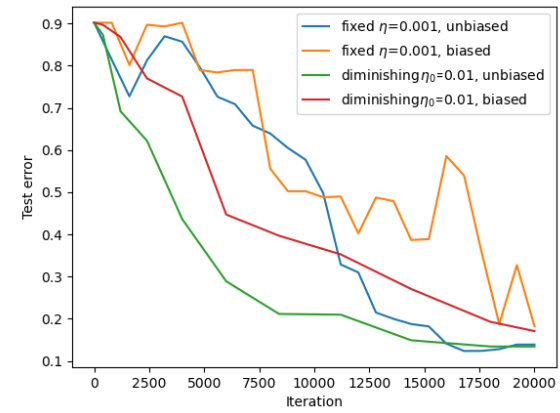


(b) Test error

Figure 2: Our asynchronous SGD for plain convex problems: (a) The Phishing data set - various step size sequences. (b) MNIST - biased and unbiased data set.



(a) Test error



(b) Test error

Figure 3: Our asynchronous SGD for non-convex problems: (a) The MNIST data set - various step size sequences. (b) MNIST - biased and unbiased data set.

Our asynchronous SGD with biased data sets: The goal of this experiment is to show that our asynchronous SGD can work well with biased (non-iid) local data sets meaning that different compute nodes use different distributions \mathcal{D}_c (contrary to all nodes using unbiased data sets such that they all have the same $\mathcal{D}_c = \mathcal{D}$ distribution). We continue with the setting as mentioned above with an adapted initial step size η_0 , see Supplemental Material D.2.4 for details. Figures 1b and 2b show no significant difference between using biased or unbiased data sets for strongly convex and plain convex problems. For the non-convex problem, Figure 3b shows that although the accuracy might fluctuate during the training process, our asynchronous SGD still achieves good accuracy in general. We conclude that our asynchronous SGD tolerates the effect of biased data sets, which is quite common in practice.

Scalability: Supplemental Material D.2.5 shows that our asynchronous SGD with linear sample size sequence scales to larger number of compute nodes. The accuracy for the same total number of gradient computations stays approximately the same and the overall execution time will reach a lower limit (where increased parallelism does not help). The linear sample size sequence gives a reduced number of communication rounds (also for an increased number of compute nodes).

6 Conclusion

We provided a tight theoretical analysis for strongly convex problems over heterogeneous local data for our asynchronous SGD with increasing sample size sequences. Experiments confirm that not only strongly convex but also plain and non-convex problems can tolerate linear increasing sample sizes – this reduces the number of communication rounds.

References

- Keith Bonawitz, Hubert Eichner, Wolfgang Grieskamp, Dzmitry Huba, Alex Ingerman, Vladimir Ivanov, Chloe Kiddon, Jakub Konecny, Stefano Mazzocchi, H Brendan McMahan, et al. Towards federated learning at scale: System design. *arXiv preprint arXiv:1902.01046*, 2019.
- Léon Bottou, Frank E. Curtis, and Jorge Nocedal. Optimization methods for large-scale machine learning. *SIAM Review*, 60(2):223–311, 2018.
- Jerry Chee and Panos Toulis. Convergence diagnostics for stochastic gradient descent with constant learning rate. In *International Conference on Artificial Intelligence and Statistics, AISTATS 2018*, pages 1476–1485, 2018.
- Jianmin Chen, Rajat Monga, Samy Bengio, and Rafal Jozefowicz. Revisiting distributed synchronous sgd. *ICLR Workshop Track*, 2016.
- Yang Chen, Xiaoyan Sun, and Yaochu Jin. Communication-efficient federated deep learning with asynchronous model update and temporally weighted aggregation. *arXiv preprint*, 2019a. URL <https://arxiv.org/pdf/1903.07424.pdf>.
- Yang Chen, Xiaoyan Sun, and Yaochu Jin. Communication-efficient federated deep learning with asynchronous model update and temporally weighted aggregation. *arXiv preprint*, 2019b. URL <https://arxiv.org/pdf/1903.07424.pdf>.
- Christopher M De Sa, Ce Zhang, Kunle Olukotun, and Christopher Ré. Taming the wild: A unified analysis of hogwild-style algorithms. In *NIPS*, pages 2674–2682, 2015.
- Kevin Hsieh, Aaron Harlap, Nandita Vijaykumar, Dimitris Konomis, Gregory R. Ganger, Phillip B. Gibbons, and Onur Mutlu. Gaia: Geo-distributed machine learning approaching LAN speeds. *14th USENIX Symposium on Networked Systems Design and Implementation (NSDI 17)*, 2017.
- Fei Wang Jie Xu, Wei Zhang. Asynchronous decentralized parallel stochastic gradient descent with differential privacy. *arXiv preprint arXiv:2008.09246*, 2020.
- Ahmed Khaled, Konstantin Mishchenko, and Peter Richtárik. Tighter theory for local sgd on identical and heterogeneous data. In *International Conference on Artificial Intelligence and Statistics*, pages 4519–4529. PMLR, 2020.
- Jakub Konečný, H Brendan McMahan, Daniel Ramage, and Peter Richtárik. Federated optimization: Distributed machine learning for on-device intelligence. *arXiv preprint arXiv:1610.02527*, 2016.
- Rémi Leblond, Fabian Pedregosa, and Simon Lacoste-Julien. Improved asynchronous parallel optimization analysis for stochastic incremental methods. *JMLR*, 19(1):3140–3207, 2018.
- Yann LeCun, Léon Bottou, Yoshua Bengio, and Patrick Haffner. Gradient-based learning applied to document recognition. *Proceedings of the IEEE*, 86(11):2278–2324, 1998.
- Tian Li, Anit Kumar Sahu, Manzil Zaheer, Maziar Sanjabi, Ameet Talwalkar, and Virginia Smith. Federated optimization for heterogeneous networks. *arXiv preprint*, 2019. URL <https://arxiv.org/pdf/1812.06127.pdf>.

- Xiangru Lian, Yijun Huang, Yuncheng Li, and Ji Liu. Asynchronous parallel stochastic gradient for nonconvex optimization. In *Advances in Neural Information Processing Systems*, pages 2737–2745, 2015.
- Xiangru Lian, Wei Zhang, Ce Zhang, and Ji Liu. Asynchronous decentralized parallel stochastic gradient descent. *arXiv preprint arXiv:1710.06952*, 2017.
- Horia Mania, Xinghao Pan, Dimitris Papailiopoulos, Benjamin Recht, Kannan Ramchandran, and Michael I Jordan. Perturbed Iterate Analysis for Asynchronous Stochastic Optimization. *SIAM Journal on Optimization*, pages 2202–2229, 2015.
- Brendan McMahan and Daniel Ramage. Federated learning: Collaborative machine learning without centralized training data, 2017. URL <https://ai.googleblog.com/2017/04/federated-learning-collaborative.html>. Last accessed 09/24/2019.
- H. Brendan McMahan, Eider Moore, Daniel Ramage, and Blaise Agüera y Arcas. Federated learning of deep networks using model averaging. *ICLR Workshop Track*, 2016.
- Qi Meng, Wei Chen, Jingcheng Yu, Taifeng Wang, Zhi-Ming Ma, and Tie-Yan Liu. Asynchronous stochastic proximal optimization algorithms with variance reduction. In *Thirty-First AAAI Conference on Artificial Intelligence*, 2017.
- Lam M. Nguyen, Phuong Ha Nguyen, Marten van Dijk, Peter Richtárik, Katya Scheinberg, and Martin Takáč. SGD and hogwild! convergence without the bounded gradients assumption. In *Proceedings of the 35th International Conference on Machine Learning, ICML 2018*, pages 3747–3755, 2018.
- Lam M. Nguyen, Phuong Ha Nguyen, Peter Richtárik, Katya Scheinberg, Martin Takáč, and Marten van Dijk. New convergence aspects of stochastic gradient algorithms. *Journal of Machine Learning Research*, 20(176):1–49, 2019a.
- P. H. Nguyen, L. M. Nguyen, and M. van Dijk. Tight dimension independent lower bound on the expected convergence rate for diminishing step sizes in SGD. *The 33th Annual Conference on Neural Information Processing Systems (NeurIPS 2019)*, 2019b.
- Benjamin Recht, Christopher Re, Stephen Wright, and Feng Niu. Hogwild: A lock-free approach to parallelizing stochastic gradient descent. In *Advances in neural information processing systems*, pages 693–701, 2011.
- Herbert Robbins and Sutton Monro. A stochastic approximation method. *The Annals of Mathematical Statistics*, 22(3): 400–407, 1951.
- Hongchao Zhang Saeed Ghadimi, Guanghui Lan. Mini-batch stochastic approximation methods for nonconvex stochastic composite optimization. *arXiv preprint arxiv:1308.6594*, 2013.
- Shaohuai Shi, Qiang Wang, Kaiyong Zhao, Zhenheng Tang, Yuxin Wang, Xiang Huang, and Xiaowen Chu. A distributed synchronous sgd algorithm with global top- k sparsification for low bandwidth networks. *arXiv preprint arXiv:1901.04359*, 2019.
- Artin Spiridonoff, Alex Olshevsky, and Ioannis Ch Paschalidis. Local sgd with a communication overhead depending only on the number of workers. *arXiv preprint arXiv:2006.02582*, 2020.
- Sebastian U Stich. Local sgd converges fast and communicates little. *arXiv preprint arXiv:1805.09767*, 2018.
- Marten Van Dijk, Lam Nguyen, Phuong Ha Nguyen, and Dzung Phan. Characterization of convex objective functions and optimal expected convergence rates for sgd. In *International Conference on Machine Learning*, pages 6392–6400, 2019.
- Luping Wang, Wei Wang, and Bo Li. Cmf1: Mitigating communication overhead for federated learning. *IEEE International Conference on Distributed Computing Systems.*, 2019.
- Cong Xie, Sanmi Koyejo, and Indranil Gupta. Asynchronous federated optimization. *arXiv preprint*, 2019. URL <https://arxiv.org/pdf/1903.03934v1.pdf>.
- Hao Yu and Rong Jin. On the computation and communication complexity of parallel sgd with dynamic batch sizes for stochastic non-convex optimization. In *International Conference on Machine Learning*, pages 7174–7183. PMLR, 2019.
- Shuxin Zheng, Qi Meng, Taifeng Wang, Wei Chen, Nenghai Yu, Zhi-Ming Ma, and Tie-Yan Liu. Asynchronous stochastic gradient descent with delay compensation. In *Proceedings of the 34th International Conference on Machine Learning-Volume 70*, pages 4120–4129. JMLR. org, 2017.
- Martin Zinkevich, John Langford, and Alex J Smola. Slow learners are fast. In *Advances in neural information processing systems*, pages 2331–2339, 2009.

Supplementary Material

A Algorithms

Algorithm 2 Initial Setup

```

1: procedure SETUP( $n$ )
2:   Initialize global model  $\hat{v}_0 = \hat{w}_{c,0,0}$  for server and compute nodes  $c \in \{1, \dots, n\}$ 
3:   Initialize diminishing round step size sequence  $\{\bar{\eta}_i\}_{i \geq 0}$ 
4:   Initialize increasing sample size sequence  $\{s_i\}_{i \geq 0}$ 
5:   for  $i \geq 0$  do
6:     for  $t \in \{0, \dots, s_i - 1\}$  do
7:       Assign  $a(i, t) = c$  with probability  $p_c$ 
8:     end for
9:     for  $c \in \{1, \dots, n\}$  do
10:       $s_{i,c} = |\{t : a(i, t) = c\}|$ 
11:    end for
12:  end for
13:       $\triangleright \{s_{i,c}\}_{i \geq 0}$  represents the sample size sequence for compute node  $c$ ; notice that  $\mathbb{E}[s_{i,c}] = p_c s_i$ 
14:  Initialize permissible delay function  $\tau(\cdot)$  with  $t - \tau(t)$  increasing in  $t$ 
15: end procedure

```

Algorithm 3 Server – Global Model

```

1: procedure ISRRECEIVE( $message$ )  $\triangleright$  Interrupt Service Routine
2:   if  $message == (i, c, U)$  is from a compute node  $c$  then  $\triangleright U$  represents  $U_{i,c}$ 
3:      $Q.enqueue(message)$   $\triangleright$  Queue  $Q$  maintains aggregate gradients not yet processed
4:   end if
5: end procedure
6:
7: procedure MAINSERVER  $\triangleright$  Represents a broadcast counter
8:    $k = 0$ 
9:    $\hat{v} = \hat{v}_0$ 
10:  Initialize  $Q$  and  $H$  to empty queues
11:  while True do
12:    if  $Q$  is not empty then
13:       $(i, c, U) \leftarrow Q.dequeue()$   $\triangleright$  Receive  $U_{i,c}$ 
14:       $\hat{v} = \hat{v} - \bar{\eta}_i \cdot U$ 
15:       $H.enqueue((i, c))$ 
16:      if  $H$  has  $(k, c)$  for all  $c \in \{1, \dots, n\}$  then
17:         $H.dequeue((k, c))$  for all  $c \in \{1, \dots, n\}$ 
18:         $k++$ 
19:        Broadcast  $(\hat{v}, k)$  to all compute nodes  $\triangleright \hat{v} = \hat{v}_k$ 
20:      end if
21:    end if
22:     $\triangleright$  Invariant:  $\hat{v} = \hat{v}_0 - \sum_{i=0}^{k-1} \sum_{c=1}^n \bar{\eta}_i U_{i,c} - \sum_{(i,c) \in H} \bar{\eta}_i U_{i,c}$ 
23:     $\triangleright \hat{v}_k$  includes the aggregate of updates  $\sum_{i=0}^{k-1} \sum_{c=1}^n \bar{\eta}_i U_{i,c}$ 
24:  end while
25: end procedure

```

Algorithm 4 ComputeNode_c – Local Model

```
1: procedure ISRRECEIVE(message) ▷ Interrupt Service Routine
2:   if message == ( $\hat{v}, k$ ) comes from the server &  $k > kold$  then
3:     ▷ The compute node will only accept and use a more fresh global model
4:     Replace the variable  $k$  as maintained by the compute node by that of message
5:      $\hat{w} = \hat{v} - \bar{\eta}_i \cdot U$  ▷ This represents  $\hat{w}_{c,i,h} = \hat{v}_k - \bar{\eta}_i \cdot U_{i,c,h}$ 
6:      $kold = k$ 
7:      $t_{delay} = s_k + \dots + s_i - (s_{i,c} - h)$ 
8:   end if
9: end procedure
10:
11: procedure MAINCOMPUTENODE( $\mathcal{D}_c$ ) ▷  $\mathcal{D}_c$  represents the local training data for compute node  $c$ 
12:    $i = 0, \hat{w} = \hat{w}_{c,0,0}$  ▷ Local round counter
13:   while True do
14:      $h = 0, U = 0$  ▷  $U_{i,c,h}$  for  $h = 0$  equals the all-zero vector
15:     while  $h < s_{i,c}$  do
16:        $t_{glob} = s_0 + \dots + s_i - (s_{i,c} - h) - 1$ 
17:        $t_{delay} = s_k + \dots + s_i - (s_{i,c} - h)$ 
18:       while  $\tau(t_{glob}) < t_{delay}$  do ▷ Invariant:  $t_{delay} \leq \tau(t_{glob})$ 
19:         only keep track of the update of  $t_{delay}$ 
20:       end while
21:       Sample uniformly at random  $\xi$  from  $\mathcal{D}_c$  ▷  $\xi$  represents  $\xi_{c,i,h}$ 
22:        $g = \nabla f(\hat{w}, \xi)$  ▷  $g$  represents  $g_{c,i,h} = \nabla f(\hat{w}_{c,i,h}, \xi_{c,i,h})$ 
23:        $U = U + g$  ▷ Represents  $U_{i,c,h+1} = U_{i,c,h} + g_{c,i,h}$  implying  $U_{i,c,h+1} = \sum_{j=0}^h g_{c,i,j}$ 
24:       Update model  $w = \hat{w} - \bar{\eta}_i \cdot g$  ▷ This represents  $w_{c,i,h+1} = \hat{w}_{c,i,h} - \bar{\eta}_i g_{c,i,h}$ 
25:       Update model  $\hat{w} = w$  ▷ This represents  $\hat{w}_{c,i,h+1} = w_{c,i,h+1}$ 
26:        $h++$ 
27:     end while
28:     Send  $(i, c, U)$  to the Server. ▷  $U$  represents  $U_{i,c} = U_{i,c,s_{i,c}} = \sum_{h=0}^{s_{i,c}-1} g_{c,i,h}$ 
29:      $i++$ 
30:   end while
31: end procedure
```

The centralized aggregation server maintains a global model which is updated according to Algorithm 3. The server receives updates from compute nodes who work on local models by executing Algorithm 4. Before any computation starts both server and clients agree on the used diminishing step size sequence, the increasing sample (mini-batch) sequences, initial default global model, and permissible delay function τ , see Algorithm 2. Note that the Interrupt Service Routines (ISR) at the compute node and server interrupt the main execution as soon as a message is received in which case the ISR routines execute before returning to the main code.

The algorithms have added comments with interpretation of the locally computed variables. These interpretations/annotations are used in next sections when proving properties.

We remark that $s_{i,c}$ are initialized by a coin flipping procedure in SETUP. Since the s_i are increasing, we may approximate $s_{i,c} \approx \mathbb{E}[s_{i,c}] = p_c s_i$ (because of the law of large numbers).

B Proofs asynchronous distributed SGD

B.1 Proof of Theorem 1

The clients in the distributed computation apply recursion (2). We want to label each recursion with an iteration count t ; this can then be used to compute with which delay function the labeled sequence $\{w_t\}$ is consistent. In order to find an ordering based on t we first define a mapping ρ from the annotated labels (c, i, h) in MAINCOMPUTENODE to t :

$$\rho(c, i, h) = \left(\sum_{l < i} s_l \right) + \min\{t' : h = |\{t \leq t' : a(i, t) = c\}|\},$$

where sequence sample size sequence $\{s_i\}$ and labelling function $a(\cdot, \cdot)$ are defined in SETUP.

Notice that given t , we can compute i as the largest index for which $\sum_{l < i} s_l \leq t$, compute $t' = t - \sum_{l < i} s_l$ and $c = a(i, t')$, and compute $h = |\{t \leq t' : a(i, t) = c\}|$. This procedure inverts ρ since $\rho(c, i, h) = t$, hence, ρ is bijective. We use ρ to order local models $\hat{w}_{c,i,h}$ by writing $\hat{w}_t = \hat{w}_{c,i,h}$ with $t = \rho(c, i, h)$. Similarly, we write $\xi_t = \xi_{c,i,h}$ for local training data samples.

From the invariant in MAINSERVER we infer that \hat{v}_k includes all the aggregate updates $U_{i,c}$ for $i < k$ and $c \in 1, \dots, n$. See Algorithm 4 for compute nodes,

$$\sum_{c \in \{1, \dots, n\}} U_{i,c} = \sum_{c \in \{1, \dots, n\}} \sum_{h=0}^{s_{i,c}-1} g_{c,i,h} \text{ with } g_{c,i,h} = \nabla f(\hat{w}_{c,i,h}; \xi_{c,i,h}).$$

By using mapping ρ , this is equal to

$$\begin{aligned} \sum_{c \in \{1, \dots, n\}} \sum_{h=0}^{s_{i,c}-1} \nabla f(\hat{w}_{c,i,h}; \xi_{c,i,h}) &= \sum_{c \in \{1, \dots, n\}} \sum_{h=0}^{s_{i,c}-1} \nabla f(\hat{w}_{\rho(c,i,h)}; \xi_{\rho(c,i,h)}) \\ &= \sum_{t=s_0+\dots+s_{i-1}}^{s_0+\dots+s_i-1} \nabla f(\hat{w}_t; \xi_t). \end{aligned}$$

This implies that \hat{v}_k includes all the gradient updates (across all clients) that correspond to \hat{w}_t for $t \leq s_0 + \dots + s_{k-1} - 1 = t_{glob} - t_{delay}$ in the notation of MAINCOMPUTENODE.

Let $\rho(c, i, h) = t$. Notice that $t = \rho(c, i, h) \leq s_0 + \dots + s_i - (s_{i,c} - h) - 1 = t_{glob}$. In MAINCOMPUTENODE we wait as long as $\tau(t_{glob}) = t_{delay}$. This means that h will not further increase until k increases in compute node c 's ISRRECEIVE when a new global model is received. This implies $t_{delay} \leq \tau(t_{glob})$ as an invariant of the algorithm. Because $t - \tau(t)$ is an increasing function in t , the derived inequality implies $t - \tau(t) \leq t_{glob} - \tau(t_{glob}) \leq t_{glob} - t_{delay}$. Notice that $\hat{w}_t = \hat{w}_{c,i,h}$ includes the updates aggregated in \hat{v}_k as last received by compute node c 's ISRRECEIVE. We concluded above that \hat{v}_k includes all gradient updates that correspond to gradient computations up to iteration count $t_{glob} - t_{delay}$. This includes gradient computations up to iteration count $t - \tau(t)$. Therefore, the computed sequence $\{\hat{w}_t\}$ is consistent with delay function τ .

As a second consequence of mapping ρ we notice that $\{\xi_t\} = \{\xi_{c,i,h}\}$. In fact $\xi_t = \xi_{c,i,h}$ for $(c, i, h) = \rho^{-1}(t)$. Notice that SETUP constructs the mapping $a(i, t) = c$ which is used to define ρ . Mapping $a(i, t)$ represents a random table of compute node assignments c generated by using a probability vector (p_1, \dots, p_n) (with c being selected with probability p_c for the (i, t) -th entry). So, $\xi_t \sim \mathcal{D}_c$ in MAINCLIENT with probability p_c . This means that $\xi_t \sim \mathcal{D}$ with $\mathcal{D} = \sum_{c=1}^n p_c \mathcal{D}_c$.

B.2 Invariant $t_{delay} \leq \tau(t_{glob})$

We propose to use increasing sample size sequences $\{s_{i,c}\}$ such that we can replace the condition $\tau(t_{glob}) < t_{delay}$ of the wait loop by $i > k + d$, where d is a threshold such that for all $i \geq d$,

$$\tau\left(\sum_{j=0}^i s_j\right) \geq 1 + \sum_{j=i-d}^i s_j. \quad (5)$$

The new wait loop guarantees that $i - k \leq d$ as an invariant of the algorithm. This implies the old invariant $t_{delay} \leq \tau(t_{glob})$ for the following reason: Let $i \geq d$. Since $t - \tau(t)$ is increasing,

$$t_{glob} - \tau(t_{glob}) \leq \sum_{j=0}^i s_j - \tau\left(\sum_{j=0}^i s_j\right) \leq \sum_{j=0}^i s_j - \left(1 + \sum_{j=i-d}^i s_j\right) = -1 + \sum_{j=0}^{i-d-1} s_j.$$

Together with $i - d \leq k$, this implies

$$\tau(t_{glob}) \geq t_{glob} - \left(-1 + \sum_{j=0}^{i-d-1} s_j\right) = s_{i-d} + \dots + s_i - (s_{i,c} - h) \geq s_k + \dots + s_i - (s_{i,c} - h) = t_{delay}.$$

This shows that the new invariant implies the old one when $i \geq d$.

B.3 Increasing sample size sequences

The following lemma shows how to construct an increasing sample size sequence given a delay function τ .

Lemma 3. *Let $g > 1$. Let function $\gamma(z)$ be increasing (i.e., $\gamma'(z) \geq 0$) and ≥ 1 for $z \geq 0$, with the additional property that $\gamma(z) \geq z\gamma'(z)\frac{g}{g-1}$ for $z \geq 0$. Suppose that*

$$\tau(x) = M_1 + \left(\frac{x + M_0}{\gamma(x + M_0)}\right)^{1/g} \text{ with } M_0 \geq \left((m + 1)\frac{g-1}{g}\right)^{g/(g-1)} \text{ and } M_1 \geq d + 2$$

for some integer $m \geq 0$ (we can choose $M_0 = 0$ if $m = 0$), and define

$$S(x) = \left(\frac{x}{\omega(x)}\frac{g-1}{g}\right)^{1/(g-1)} \text{ with } \omega(x) = \gamma\left(\left(\frac{x}{g}\right)^{g/(g-1)}\right).$$

Then $s_i = \lceil \frac{1}{d+1}S(\frac{m+i+1}{d+1}) \rceil$ satisfies property (5) (i.e., (3)).

The lemma simplifies to Lemma 1 if we use $\gamma(z) = 1$.

Proof. Since $\gamma(z)$ is increasing and ≥ 1 for $z \geq 0$, also $\omega(x)$ is increasing and ≥ 1 for $x \geq 0$ (notice that $g > 1$).

We also want to show that $z/\omega(z)$ is increasing for $z \geq 0$. Its derivative is equal to

$$\frac{1}{\omega(z)}\left(1 - \frac{z\omega'(z)}{\omega(z)}\right)$$

which is ≥ 0 if $\omega(z) \geq z\omega'(z)$ (because $\omega(z)$ is positive). The latter is equivalent (by ω 's definition) to

$$\gamma\left(\left(\frac{z}{g}\right)^{g/(g-1)}\right) \geq z\gamma'\left(\left(\frac{z}{g}\right)^{g/(g-1)}\right)\frac{g}{g-1}\left(\frac{z}{g}\right)^{g/(g-1)-1}\frac{g-1}{g}.$$

This is implied by $\gamma(y) \geq y\gamma'(y)\frac{g}{g-1}$ for $y = \left(\frac{z}{g}\right)^{g/(g-1)}$. From our assumptions on $\gamma(z)$ we infer that this is true.

Since $x/\omega(x)$ is increasing, also $S(x)$ is increasing for $x \geq 0$. This implies

$$\begin{aligned} \sum_{j=0}^i s_j &= \sum_{j=0}^i \lceil \frac{1}{d+1}S(\frac{m+j+1}{d+1}) \rceil \geq \sum_{j=m}^{i+m} \frac{1}{d+1}S(\frac{j+1}{d+1}) \\ &= \sum_{j=0}^{i+m} \frac{1}{d+1}S(\frac{j+1}{d+1}) - \sum_{j=0}^{m-1} \frac{1}{d+1}S(\frac{j+1}{d+1}) \\ &\geq \int_{z=0}^{m+i+1} \frac{1}{d+1}S(\frac{z}{d+1})dz - \int_{z=0}^{m+1} \frac{1}{d+1}S(\frac{z}{d+1})dz \\ &= \int_{z=0}^{(m+i+1)/(d+1)} S(z)dz - \int_{z=0}^{(m+1)/(d+1)} S(z)dz. \end{aligned}$$

Since $\omega(z) \geq 1$,

$$\int_{z=0}^{(m+1)/(d+1)} S(z)dz \leq \int_{z=0}^{(m+1)/(d+1)} \left(\frac{z}{g}\right)^{1/(g-1)} dz = \left(\frac{m+1}{d+1}\right) \cdot \frac{g-1}{g} \leq M_0.$$

Let $x = (m+i+1)/(d+1)$. Then,

$$\sum_{j=0}^i s_j \geq \int_{z=0}^x S(z)dz - M_0.$$

Because $\omega(z)$ is increasing for $z \geq 0$ we have

$$\int_{z=0}^x S(z)dz \geq \frac{1}{\omega(x)^{1/(g-1)}} \cdot \int_{z=0}^x \left(\frac{z}{g}\right)^{1/(g-1)} dz = \frac{1}{\omega(x)^{1/(g-1)}} \cdot \left(\frac{x}{g}\right)^{g/(g-1)}.$$

Since $x/\gamma(x)$ is increasing (its derivative is equal to $\frac{1}{\gamma(x)}\left(1 - \frac{x\gamma'(x)}{\gamma(x)}\right)$ and is positive by our assumptions on $\gamma(x)$), also $\tau(x)$ is increasing and we infer

$$\tau\left(\sum_{j=0}^i s_j\right) \geq \tau\left(\int_{z=0}^x S(z)dz - M_0\right) \geq \tau\left(\frac{1}{\omega(x)^{1/(g-1)}} \cdot \left(\frac{x}{g}\right)^{g/(g-1)} - M_0\right).$$

By τ 's definition, the right hand side is equal to

$$M_1 + \frac{\left(\frac{1}{\omega(x)^{1/(g-1)}} \left(x \frac{g-1}{g}\right)^{g/(g-1)}\right)^{1/g}}{\gamma\left(\frac{1}{\omega(x)^{1/(g-1)}} \cdot \left(x \frac{g-1}{g}\right)^{g/(g-1)}\right)^{1/g}}. \quad (6)$$

Since $S(x)$ is increasing, we have

$$\begin{aligned} 1 + \sum_{j=i-d}^i s_j &= 1 + \sum_{j=i-d}^i \left\lceil \frac{1}{d+1} S\left(\frac{m+j+1}{d+1}\right) \right\rceil \leq 1 + (d+1) \left\lceil \frac{1}{d+1} S\left(\frac{m+i+1}{d+1}\right) \right\rceil \\ &\leq d+2 + S\left(\frac{m+i+1}{d+1}\right) = d+2 + S(x). \end{aligned}$$

Since $M_1 \geq d+2$, the right hand side is at most (6) if

$$\frac{\left(\frac{1}{\omega(x)^{1/(g-1)}} \left(x \frac{g-1}{g}\right)^{g/(g-1)}\right)^{1/g}}{\gamma\left(\frac{1}{\omega(x)^{1/(g-1)}} \cdot \left(x \frac{g-1}{g}\right)^{g/(g-1)}\right)^{1/g}} \geq \left(\frac{x}{\omega(x)} \frac{g-1}{g}\right)^{1/(g-1)} = S(x).$$

After raising to the power g and reordering terms this is equivalent to

$$\omega(x) \geq \gamma\left(\frac{1}{\omega(x)^{1/(g-1)}} \cdot \left(x \frac{g-1}{g}\right)^{g/(g-1)}\right).$$

Since $\omega(x) \geq 1$ and $\gamma(z)$ is increasing, this is implied by

$$\omega(x) \geq \gamma\left(\left(x \frac{g-1}{g}\right)^{g/(g-1)}\right).$$

Since this is true by the definition of $\omega(x)$, we obtain inequality (5).

B.4 Diminishing step size sequences

We assume the sample size sequence $s_i = \left\lceil \frac{1}{d+1} S\left(\frac{m+i+1}{d+1}\right) \right\rceil$ developed in the previous subsection:

Lemma 4. *We assume the sample size sequence $s_i = \left\lceil \frac{1}{d+1} S\left(\frac{m+i+1}{d+1}\right) \right\rceil$ of Lemma 3. Let $\{E_t\}$ be a constant or increasing sequence with $E_t \geq 1$. For $i \geq 0$, we define*

$$\bar{E}_i = E_{\sum_{j=0}^i s_j}.$$

We define $\bar{E}_{-1} = E_0$ and assume for $i \geq 0$ that

$$\bar{E}_i \leq 2\bar{E}_{i-1} \text{ and } s_0 - 1 \leq E_0.$$

Let $q \geq 0$, and a_0 and a_1 be constants such that

$$a_1 = a_0 \cdot \max\left\{3, \left(1 + \frac{m+2}{m+1}\right)^{1/(g-1)}\right\}^q.$$

For $g \geq 2$ and $q \leq 1$ this implies $a_0 \leq a_1 \leq 3 \cdot a_0$.

Then the diminishing step size sequence $\eta_t = \frac{\alpha_t}{\mu(t+E_t)^q}$ with parameters $\{\alpha_t\}$ defined by

$$\eta_t = \frac{\alpha_t}{\mu(t+E_t)^q} = \frac{a_0}{\mu\left(\left(\sum_{j=0}^{i-1} s_j\right) + \bar{E}_{i-1}\right)^q} \stackrel{\text{DEF}}{=} \bar{\eta}_i$$

for $t \in \left\{\left(\sum_{j=0}^{i-1} s_j\right), \dots, \left(\sum_{j=0}^{i-1} s_j\right) + s_i - 1\right\}$ and $i \geq 0$ satisfies

$$a_0 = \alpha_0 \leq \alpha_t \leq a_1.$$

Notice that Lemma 2 describes the case $g \geq 2$ and $q \leq 1$ in a different wording (by defining a set \mathcal{Z} of step size sequences).

Proof. For $i \geq 1$, we first show a relation between s_i and s_{i-1} (notice that ω is increasing):

$$\begin{aligned}
s_i - 1 &\leq \frac{1}{d+1} S\left(\frac{m+i+1}{d+1}\right) = \frac{1}{d+1} \left(\frac{1}{\omega\left(\frac{m+i+1}{d+1}\right)} \frac{m+i+1}{d+1} \frac{g-1}{g}\right)^{1/(g-1)} \\
&\leq \frac{1}{d+1} \left(\frac{1}{\omega\left(\frac{m+i}{d+1}\right)} \frac{m+i+1}{d+1} \frac{g-1}{g}\right)^{1/(g-1)} \\
&= \left(\frac{m+i+1}{m+i}\right)^{1/(g-1)} \frac{1}{d+1} \left(\frac{1}{\omega\left(\frac{m+i}{d+1}\right)} \frac{m+i}{d+1} \frac{g-1}{g}\right)^{1/(g-1)} \\
&= \left(\frac{m+i+1}{m+i}\right)^{1/(g-1)} \frac{1}{d+1} S\left(\frac{m+i}{d+1}\right) \leq \left(\frac{m+2}{m+1}\right)^{1/(g-1)} s_{i-1}
\end{aligned} \tag{7}$$

For $i \geq 1$ and $t \in \{(\sum_{j=0}^{i-1} s_j), \dots, (\sum_{j=0}^{i-1} s_j) + s_i - 1\}$, we are now able to derive a bound

$$\begin{aligned}
\alpha_t &= a_0 \frac{(t + E_t)^q}{((\sum_{j=0}^{i-1} s_j) + \bar{E}_{i-1})^q} \leq a_0 \left(\frac{(\sum_{j=0}^i s_j) - 1 + \bar{E}_i}{(\sum_{j=0}^{i-1} s_j) + \bar{E}_{i-1}}\right)^q \\
&\leq a_0 \left(\frac{(\sum_{j=0}^i s_j) - 1 + 2\bar{E}_{i-1}}{(\sum_{j=0}^{i-1} s_j) + \bar{E}_{i-1}}\right)^q = a_0 \left(1 + \frac{s_i - 1 + \bar{E}_{i-1}}{(\sum_{j=0}^{i-1} s_j) + \bar{E}_{i-1}}\right)^q \\
&\leq a_0 \left(1 + \frac{((m+2)/(m+1))^{1/(g-1)} s_{i-1} + \bar{E}_{i-1}}{(\sum_{j=0}^{i-1} s_j) + \bar{E}_{i-1}}\right)^q \\
&\leq a_0 \left(1 + \frac{((m+2)/(m+1))^{1/(g-1)} (\sum_{j=0}^{i-1} s_j) + \bar{E}_{i-1}}{(\sum_{j=0}^{i-1} s_j) + \bar{E}_{i-1}}\right)^q \\
&\leq a_0 \left(1 + \left(\frac{m+2}{m+1}\right)^{1/(g-1)}\right)^q.
\end{aligned}$$

Notice that for $g \geq 2$ and $q \leq 1$, this bound is at most $3 \cdot a_0$.

We still need to analyse the case $i = 0$. This gives the bound (notice that $s_0 - 1 \leq E_0$ and $\bar{E}_0 \leq 2\bar{E}_{-1} = 2E_0$)

$$\alpha_t = a_0 \frac{(t + E_t)^q}{((\sum_{j=0}^{i-1} s_j) + E_0)^q} = a_0 \frac{(t + E_t)^q}{E_0^q} \leq a_0 \frac{(s_0 - 1 + \bar{E}_0)^q}{E_0^q} \leq a_0 \cdot 3^q.$$

The step size for iteration t is equal to

$$\eta_t = \frac{\alpha_t}{\mu(t + E_t)^q} = \frac{a_0}{\mu((\sum_{j=0}^{i-1} s_j) + \bar{E}_{i-1})^q},$$

hence, $\alpha_0 = a_0$.

C Analysis general recursion

The optimization problem for training many Machine Learning (ML) models using a training set $\{\xi_i\}_{i=1}^M$ of M samples can be formulated as a finite-sum minimization problem as follows

$$\min_{w \in \mathbb{R}^d} \left\{ F(w) = \frac{1}{M} \sum_{i=1}^M f(w; \xi_i) \right\}. \tag{8}$$

The objective is to minimize a loss function with respect to model parameters w . This problem is known as empirical risk minimization and it covers a wide range of convex and non-convex problems from the ML domain, including, but not limited to, logistic regression, multi-kernel learning, conditional random fields and neural networks. We are interested in solving the following more general stochastic optimization problem with respect to some distribution \mathcal{D} :

$$\min_{w \in \mathbb{R}^d} \{F(w) = \mathbb{E}_{\xi \sim \mathcal{D}}[f(w; \xi)]\}, \tag{9}$$

where F has a Lipschitz continuous gradient and f has a *finite lower bound* for every ξ .

The general form (9) can be solved by using SGD as described in Algorithm 5. Thanks to its simplicity in implementation and efficiency in dealing with large scale data sets, stochastic gradient descent, originally introduced in [Robbins and Monro, 1951], has become the method of choice for solving not only (8) when m is large but also (9).

Algorithm 5 Stochastic Gradient Descent (SGD) Method

```

1: Initialize:  $w_0$ 
2: Iterate:
3: for  $t = 0, 1, 2, \dots$  do
4:   Choose a step size (i.e., learning rate)  $\eta_t > 0$ .
5:   Generate a random variable  $\xi_t$ .
6:   Compute a stochastic gradient  $\nabla f(w_t; \xi_t)$ .
7:   Update the new iterate  $w_{t+1} = w_t - \eta_t \nabla f(w_t; \xi_t)$ .
8: end for

```

C.1 The Hogwild! algorithm

To speed up SGD, an asynchronous SGD known as Hogwild! was introduced in [Recht et al., 2011]. Here, multiple computing threads work together and update shared memory in asynchronous fashion. The shared memory stores the most recently computed weight as a result of the SGD iterations computed by each of the computing threads. Writes to and reads from vector positions in shared memory can be inconsistent. As a result a computing thread may start reading positions of the current weight vector from shared memory while these positions are updated by other computing threads out-of-order. Only writes to and reads from shared memory positions are considered atomic. This means that, when a computing thread reads the ‘current’ weight vector from shared memory, this weight vector is a mix of partial updates to the weight vector from other computing threads that executed previous SGD iterations.

[Nguyen et al., 2018, 2019a] introduce a general recursion for w_t . The recursion explains which positions in w_t should be updated in order to compute w_{t+1} . Since w_t is stored in shared memory and is being updated in a possibly non-consistent way by multiple cores who each perform recursions, the shared memory will contain a vector w whose entries represent a mix of updates. That is, before performing the computation of a recursion, a computing thread will first read w from shared memory, however, while reading w from shared memory, the entries in w are being updated out of order. The final vector \hat{w}_t read by the computing thread represents an aggregate of a mix of updates in previous iterations.

The general recursion (parts of text extracted from [Nguyen et al., 2019a]) is defined as follows: For $t \geq 0$,

$$w_{t+1} = w_t - \eta_t d_{\xi_t} S_{u_t}^{\xi_t} \nabla f(\hat{w}_t; \xi_t), \quad (10)$$

where

- \hat{w}_t represents the vector used in computing the gradient $\nabla f(\hat{w}_t; \xi_t)$ and whose entries have been read (one by one) from an aggregate of a mix of previous updates that led to w_j , $j \leq t$, and
- the $S_{u_t}^{\xi_t}$ are diagonal 0/1-matrices with the property that there exist real numbers d_{ξ} satisfying

$$d_{\xi} \mathbb{E}[S_u^{\xi} | \xi] = D_{\xi}, \quad (11)$$

where the expectation is taken over u and D_{ξ} is the diagonal 0/1 matrix whose 1-entries correspond to the non-zero positions in $\nabla f(w; \xi)$ in the following sense: The i -th entry of D_{ξ} ’s diagonal is equal to 1 if and only if there exists a w such that the i -th position of $\nabla f(w; \xi)$ is non-zero.

The role of matrix $S_{u_t}^{\xi_t}$ is that it filters which positions of gradient $\nabla f(\hat{w}_t; \xi_t)$ play a role in (10) and need to be computed. Notice that D_{ξ} represents the support of $\nabla f(w; \xi)$; by $|D_{\xi}|$ we denote the number of 1s in D_{ξ} , i.e., $|D_{\xi}|$ equals the size of the support of $\nabla f(w; \xi)$.

We restrict ourselves to choosing (i.e., fixing a-priori) *non-empty* matrices S_u^{ξ} that ‘partition’ D_{ξ} in D approximately ‘equally sized’ S_u^{ξ} :

$$\sum_u S_u^{\xi} = D_{\xi},$$

where each matrix S_u^{ξ} has either $\lfloor |D_{\xi}|/D \rfloor$ or $\lceil |D_{\xi}|/D \rceil$ ones on its diagonal. We uniformly choose one of the matrices S_u^{ξ} in (10), hence, d_{ξ} equals the number of matrices S_u^{ξ} , see (11).

In order to explain recursion (10) we consider two special cases. For $D = \bar{\Delta}$, where

$$\bar{\Delta} = \max_{\xi} \{|D_{\xi}|\}$$

represents the maximum number of non-zero positions in any gradient computation $f(w; \xi)$, we have that for all ξ , there are exactly $|D_\xi|$ diagonal matrices S_u^ξ with a single 1 representing each of the elements in D_ξ . Since $p_\xi(u) = 1/|D_\xi|$ is the uniform distribution, we have $\mathbb{E}[S_u^\xi | \xi] = D_\xi/|D_\xi|$, hence, $d_\xi = |D_\xi|$. This gives the recursion

$$w_{t+1} = w_t - \eta_t |D_{\xi_t}| [\nabla f(\hat{w}_t; \xi_t)]_{u_t}, \quad (12)$$

where $[\nabla f(\hat{w}_t; \xi_t)]_{u_t}$ denotes the u_t -th position of $\nabla f(\hat{w}_t; \xi_t)$ and where u_t is a uniformly selected position that corresponds to a non-zero entry in $\nabla f(\hat{w}_t; \xi_t)$.

At the other extreme, for $D = 1$, we have exactly one matrix $S_1^\xi = D_\xi$ for each ξ , and we have $d_\xi = 1$. This gives the recursion

$$w_{t+1} = w_t - \eta_t \nabla f(\hat{w}_t; \xi_t). \quad (13)$$

Recursion (13) represents Hogwild!. In a single-thread setting where updates are done in a fully consistent way, i.e. $\hat{w}_t = w_t$, yields SGD.

Algorithm 6 gives the pseudo code corresponding to recursion (10) with our choice of sets S_u^ξ (for parameter D).

Algorithm 6 Hogwild! general recursion

```

1: Input:  $w_0 \in \mathbb{R}^d$ 
2: for  $t = 0, 1, 2, \dots$  in parallel do
3:   read each position of shared memory  $w$  denoted by  $\hat{w}_t$  (each position read is atomic)
4:   draw a random sample  $\xi_t$  and a random “filter”  $S_{u_t}^{\xi_t}$ 
5:   for positions  $h$  where  $S_{u_t}^{\xi_t}$  has a 1 on its diagonal do
6:     compute  $g_h$  as the gradient  $\nabla f(\hat{w}_t; \xi_t)$  at position  $h$ 
7:     add  $\eta_t d_{\xi_t} g_h$  to the entry at position  $h$  of  $w$  in shared memory (each position update is atomic)
8:   end for
9: end for

```

In order to use Algorithm 6 in our asynchronous SGD setting where local compute nodes compute SGD iterations on local data sets, we use the following reinterpretation of shared memory and computing threads. Compute nodes represent the different computing threads. The centralized server plays the role of shared memory where locally computed weight vectors at the compute nodes are ‘aggregated’ as in (10). Each ComputeNode_c first reads each of the entries of the weight vector w currently stored at the compute node itself. This weight vector w includes local updates (due to SGD iterations at the compute node itself) as well as updates from other compute nodes since w originally came from the server when transmitting the global model in a broadcast message. Therefore, ComputeNode_c reads a \hat{w}_t that can be interpreted as a series of successive atomic reads from shared memory w as described above. Next the gradient $\nabla f(\hat{w}_t; \xi_t)$ for some sample $\xi_t \sim \mathcal{D}_c$ is computed. Since the order in which compute nodes are executing their SGD iterations is determined by probabilities $\{p_c\}$, this means that from a higher abstraction level $\nabla f(\hat{w}_t; \xi_t)$ for some sample $\xi_t \sim \mathcal{D}$ is computed (that is, with probability p_c sample $\xi_t \sim \mathcal{D}_c$ and ComputeNode_c is the one executing the corresponding SGD iteration). The gradient multiplied by a step size η_t and correction factor d_{ξ_t} is subtracted from the weight vector stored at the server (after it receives the local update from the compute node). This is done by a series of successive atomic writes. Each of the compute nodes (just like the computing threads above) work in parallel continuously updating entries in the weight vector w stored at the server (and stored locally at each compute node).

In the context of different computing threads atomically reading and writing entries of vector w from shared memory, we define the amount of asynchronous behavior by parameter τ as in [Nguyen et al., 2019a]:

Definition 2. *We say that weight vector w stored at the server is consistent with delay τ with respect to recursion (10) if, for all t , vector \hat{w}_t includes the aggregate of the updates up to and including those made during the $(t - \tau)$ -th iteration (where (10) defines the $(t + 1)$ -st iteration). Each position read from shared memory is atomic and each position update to shared memory is atomic (in that these cannot be interrupted by another update to the same position).*

Even though this (original) definition does not consider τ as a function of the iteration count t , the next subsections do summarize how τ can depend as a function on t .

C.2 Convergence rate for strongly convex problems

In this section we let f be L -smooth, convex, and let the objective function $F(w) = \mathbb{E}_{\xi \sim \mathcal{D}}[f(w; \xi)]$ be μ -strongly convex with finite $N = 2\mathbb{E}[\|\nabla f(w_*; \xi)\|^2]$ where $w_* = \arg \min_w F(w)$. Notice that we do not assume the bounded gradient assumption which assumes $\mathbb{E}[\|\nabla f(w; \xi)\|^2]$ is bounded for all $w \in \mathbb{R}^d$ (not only $w = w_*$ as in Assumption 4) and is in conflict with assuming strong convexity as explained in [Nguyen et al., 2018, 2019a].

C.2.1 Constant step sizes

Algorithm 6 for $D = 1$ corresponds to Hogwild! with recursion (13). For finite-sum problems, [Leblond et al., 2018] proves for constant step sizes $\eta_t = \eta = \frac{a}{L}$ with delay

$$\tau \leq \frac{1}{\eta\mu} \quad (14)$$

and parameter $a \leq (5(1 + 2\tau\sqrt{\Delta})\sqrt{1 + \frac{\mu}{2L} \min\{\frac{1}{\sqrt{\Delta}}, \tau\}})^{-1}$ as a function of τ , where Δ measures sparsity according to Definition 7 in [Leblond et al., 2018], that the convergence rate $\mathbb{E}[\|\hat{w}_t - w_*\|^2]$ is at most

$$\mathbb{E}[\|\hat{w}_t - w_*\|^2] \leq 2(1 - \rho)^t \|w_0 - w_*\|^2 + b,$$

where $\rho = \frac{aL}{\mu}$ and $b = (\frac{4\eta(C_1 + \tau C_2)}{\mu} + 2\eta^2 C_1 \tau)N$ for $C_1 = 1 + \sqrt{\Delta}\tau$ and $C_2 = \sqrt{\Delta} + \eta\mu C_1$.

With a fixed learning rate $\eta_t = \eta$, SGD and Hogwild! may provide fast initial improvement, after which it oscillates within a region containing a solution [Bottou et al., 2018, Chee and Toulis, 2018]. The upper bound on the convergence rate shows that convergence is to within some range of the optimal value; we have $\mathbb{E}[\|\hat{w}_t - w_*\|^2] = \mathcal{O}(\eta)$.

Hence, SGD and Hogwild! can fail to converge to a solution. It is known that the behavior of SGD is strongly dependent on the chosen learning rate and on the variance of the stochastic gradients. To overcome this issue, there are two main lines of research that have been proposed in literature: variance reduction methods and diminishing learning rate schemes. These algorithms guarantee to converge to the optimal value.

Upper bound (14) allows us to set the maximal sample size $s = s_i$ in terms of the amount of asynchronous behavior allowed by d in (5). This allows an informed decision on how to reduce the number of broadcast messages as much as possible. We need $\tau = (d + 1)s \leq \frac{1}{\eta\mu}$, i.e., $s \leq \frac{1}{\eta\mu(d+1)} = \frac{a}{L\mu(d+1)}$ which is typically large.

C.2.2 Diminishing step sizes

We slightly reformalize^l Lemma 11 from [Nguyen et al., 2018]:

Lemma 5. [Nguyen et al., 2018, 2019a] Let $\tau(t)$ be a delay function satisfying $2L\alpha/\mu \leq \tau(t) \leq t$ with the additional property that there exists a constant T_1 such that for large enough $t \geq T_1$, $\tau(t) \leq \sqrt{\frac{t}{\ln t}} \cdot (1 - \frac{1}{\ln t})$. Let

$$\{\eta_t = \frac{\alpha_t}{\mu(t + 2\tau(t))}\}$$

be a step size sequence with $12 \leq \alpha_t \leq \alpha$. Then the expected convergence rates satisfy

$$\begin{aligned} \mathbb{E}[\|\hat{w}_{t+1} - w_*\|^2] &\leq \frac{4\alpha^2 DN}{\mu^2} \frac{1}{t} + \mathcal{O}\left(\frac{1}{t \ln t}\right) \text{ and} \\ \mathbb{E}[\|w_{t+1} - w_*\|^2] &\leq \frac{4\alpha^2 DN}{\mu^2} \frac{1}{t} + \mathcal{O}\left(\frac{1}{t \ln t}\right). \end{aligned}$$

We apply Lemma 5 for $D = 1$ which corresponds to Hogwild! as applied in this paper.

The conditions of Lemma 3 are satisfied for $g = 2$ and $\gamma(z) = 4 \ln z$. Let

$$M_1 = \max \left\{ d + 2, \frac{2L\alpha}{\mu}, \frac{1}{2} \left[\frac{m + 1}{16(d + 1)^2} \frac{1}{\ln(\frac{m+1}{2(d+1)})} \right] \right\}$$

and

$$M_0 = \left((m + 1) \frac{g - 1}{g} \right)^{g/(g-1)} = \frac{(m + 1)^2}{4}.$$

^lThe original lemma requires $2L\alpha/\mu \leq \tau(t) \leq \sqrt{\frac{t}{\ln t}} \cdot (1 - \frac{1}{\ln t})$ which cannot be realized for small t . Nevertheless, if $\tau(t) \leq \sqrt{\frac{t}{\ln t}} \cdot (1 - \frac{1}{\ln t})$ for $t \geq T_1$ where T_1 is a constant, then the derivation after (47) in [Nguyen et al., 2018] still holds true if we consider $\sum_{i=T_1}^t a_i \tau(i)^2$ and $\sum_{i=T_1}^t a_i \tau(i)$, respectively. We can replace the sums $\sum_{i=1}^{T_1} a_i \tau(i)^2$ and $\sum_{i=1}^{T_1} a_i \tau(i)$ by $\mathcal{O}(1)$ terms and as a result the derivations that lead to Lemma 11 still follow.

This defines

$$\tau(t) = M_1 + \left(\frac{t + M_0}{\gamma(t + M_0)} \right)^{1/g} = M_1 + \sqrt{\frac{t + M_0}{4 \ln(t + M_0)}}.$$

For t large enough such that both $t \geq \max\{M_0, e^3\}$ and $(1 - \sqrt{3/4}) \cdot \sqrt{(t + M_0)/\ln(t + M_0)} \geq M_1$, $\tau(t) \leq \sqrt{(t/\ln t) \cdot (1 - 1/\ln t)}$ for the following reason: The square root

$$\sqrt{\frac{t + M_0}{4 \ln(t + M_0)}} \leq \sqrt{\frac{3}{4} \frac{t}{\ln t} \cdot \left(1 - \frac{1}{\ln t}\right)}$$

because $1 - 1/\ln t \geq 2/3$ and $(t + M_0)/\ln(t + M_0) \leq (t + M_0)/\ln t \leq 2t/\ln t$. Adding the bound on M_1 completes the argument. Hence, we can apply Lemma 5. We use Lemma 3 to obtain a concrete sample size sequence $\{s_i\}$. This leads to an increasing sample size sequence defined by

$$s_i = \lceil \frac{m + i + 1}{16(d + 1)^2} \frac{1}{\ln(\frac{m+i+1}{2(d+1)})} \rceil = O\left(\frac{i}{\ln i}\right).$$

(For example, $s_0 = \lceil 31.989/(d + 1) \rceil$ corresponds to $m + 1 = 2(d + 1) \cdot 1937$. For $d = 1$, this gives $s_0 = 16$.)

By setting $E_t = 2\tau(t)$ in the step size sequence based on $\{\eta_t\}$ of Lemma 5, we can apply our recipe of Lemma 4 for computing the round step size sequence $\{\bar{\eta}_i\}$. Notice that we need to choose $a_0 = 12$ and $\alpha = a_1 \leq 3 \cdot a_0 = 36$ in Lemma 4; we use $\alpha = 36$ in the formulas below. Also notice that $E_0 = 2\tau(0) \geq s_0$ by the definitions of s_0 , M_1 and $\tau(t)$.

The inequality $\bar{E}_{i+1} \leq 2\bar{E}_i$ follows from (remember $E_t = 2\tau(t)$)

$$\sqrt{\frac{\sum_{j=0}^i s_j + M_0}{4 \ln(\sum_{j=0}^i s_j + M_0)}} \leq 2 \sqrt{\frac{\sum_{j=0}^{i-1} s_j + M_0}{4 \ln(\sum_{j=0}^{i-1} s_j + M_0)}}.$$

Notice that (7) for $g = 2$ implies $s_i - 1 \leq 2s_{i-1}$. Since $s_{i-1} \geq 1$ we have $s_i \leq 3s_{i-1}$. We derive

$$\begin{aligned} \sqrt{\frac{\sum_{j=0}^i s_j + M_0}{4 \ln(\sum_{j=0}^i s_j + M_0)}} &\leq \sqrt{\frac{\sum_{j=0}^i s_j + M_0}{4 \ln(\sum_{j=0}^{i-1} s_j + M_0)}} \leq \sqrt{\frac{\sum_{j=0}^{i-1} s_j + 3s_{i-1} + M_0}{4 \ln(\sum_{j=0}^{i-1} s_j + M_0)}} \\ &\leq \sqrt{\frac{4(\sum_{j=0}^{i-1} s_j + M_0)}{4 \ln(\sum_{j=0}^{i-1} s_j + M_0)}} = 2 \sqrt{\frac{\sum_{j=0}^{i-1} s_j + M_0}{4 \ln(\sum_{j=0}^{i-1} s_j + M_0)}}. \end{aligned}$$

It remains to show that $\bar{E}_1 \leq 2E_0 = 2\bar{E}_{-1}$. This follows from a similar derivation as the one above if we can show that $s_0 \leq 3M_0$. The latter is indeed true because $\frac{1}{16(d+1)^2} \leq \frac{1}{16} \leq \frac{3}{4} \leq 3 \frac{m+1}{4}$.

Now we are ready to apply Lemma 4 from which we obtain diminishing round step size sequence defined by

$$\bar{\eta}_i = \frac{12}{\mu} \cdot \frac{1}{\sum_{j=0}^{i-1} s_j + 2M_1 + \sqrt{\frac{(m+1)^2/4 + \sum_{j=0}^{i-1} s_j}{\ln((m+1)^2/4 + \sum_{j=0}^{i-1} s_j)}}} = O\left(\frac{\ln i}{i^2}\right).$$

Application of Lemma 5 proves *Theorem 2* (in the main body).

C.2.3 Tightness

For first order stochastic algorithms the best attainable convergence rate for t is at least $\frac{1}{2} \frac{N}{\mu^2} \frac{1}{t} (1 - O((\ln t)/t))$ as shown in [Nguyen et al., 2019b]. This means that for increasing t the upper bound on the expected convergence rate of Lemma 5 converges to factor $\leq 2 \cdot 4 \cdot 36^2 = 10368$ times the best attainable convergence rate.

The factor 10368 can be improved to a smaller value: The component 36 comes from $3a_0$ where the factor 3 follows from coarse upper bounding in the proof of Lemma 4.

Discussion on how fast the upper bound gets close to within a constant factor of the best attainable convergence rate: The $O(1/(t \ln t))$ term in the upper bound and $O((\ln t)/t)$ term in the lower bound (given by the best attainable

convergence rate) converges to 0, but how fast? Some indication follows from analysis provided in [Nguyen et al., 2018] where is stated that if $\tau(t)$ is set to meet the upper bound $\sqrt{(t/\ln t) \cdot (1 - 1/\ln t)}$, then for large enough

$$t \geq T_0 = \exp\left[2\sqrt{\Delta}\left(1 + \frac{(L + \mu)\alpha}{\mu}\right)\right]$$

the constants of all the asymptotic higher order terms in $O(1/(t \ln t))$ in the upper bound on the convergence rate that contain $\tau(t)$ are such that the concrete values of all these terms are at most the leading explicit term of the upper bound on the convergence rate.** So, for $t \geq T_0$, we have that the upper bound on the convergence rate starts to look like 2 (or a small factor) times the leading explicit term without the asymptotic $O(1/(t \ln t))$ term. This gives an indication when the upper bound starts to get close to $2 \cdot 4 \cdot 36^2$ times the best attainable convergence rate.

Our recipe in Lemma 1 for computing a sample size sequence $\{s_i\}$ can be applied for a smaller delay function, e.g., $\tau(t) = t^{1/3}$. For such a new sample size sequence we can repeat the same type of calculations as presented in this subsection and show how the diminishing round step size sequence computed according to our recipe in Lemma 4 can still achieve an $O(1/t)$ upper bound on the convergence rate which itself converges within a constant factor of the best attainable convergence rate. This convergence sets in for $t \geq T_0$ where T_0 corresponds to $\tau(t) = t^{1/3}$. The new T_0 is expected to be significantly smaller. So, the $O(1/t)$ convergence rate sooner gets close to within a constant factor of the best attainable convergence rate if we use a less increasing sample size sequence. In theory this means (1) less rounds because the convergence rate diminishes faster, hence, a smaller number K of total gradient computations is needed. And (2), this means more rounds because the sample sizes are chosen smaller while still a total number of K gradient computations are needed for the desired convergence. It is an open problem to find the right theoretical balance. In experiments, however, we see that even with linear increasing sample size sequences we attain (fast) practical convergence. So, the offered theoretical analysis in this subsection should be used as an understanding that using a (linearly) increasing sample size sequence is a promising design trick; experiments show practical convergence not only for strongly convex problems but also for plain and non-convex problems.

C.3 Plain convex and non-convex problems

For an objective function F (as defined in (1)), we are generally interested in the expected convergence rate

$$Y_t^{(F)} = \mathbb{E}[F(w_t) - F_*],$$

where $F_* = F(w_*)$ for a global minimum w_* (and the expectation is over the randomness used in the recursive computation of w_t by the probabilistic optimization algorithm of our choice). This implicitly assumes that there exists a global minimum w_* , i.e., $\mathcal{W}^* = \{w_* \in \mathbb{R}^d : \forall w \in \mathbb{R}^d F(w_*) \leq F(w)\}$ defined as the set of all w_* that minimize $F(\cdot)$ is non-empty. Notice that \mathcal{W}^* can have multiple global minima even for convex problems.

For convex problems a more suitable definition for Y_t is the averaged expected convergence rate defined as

$$Y_t^{(A)} = \frac{1}{t+1} \sum_{i=t+1}^{2t} \mathbb{E}[F(w_i) - F_*]$$

and for strongly convex objective functions we may use

$$Y_t^{(w)} = \mathbb{E}[\inf\{\|w_t - w_*\|^2 : w_* \in \mathcal{W}^*\}].$$

The ω -convex objective functions define a range of functions between plain convex and strongly convex for which both convergence rate definitions can be computed for diminishing step sizes [Van Dijk et al., 2019]. From [Van Dijk et al., 2019] we have that an objective function with 'curvature' $h \in [0, 1]$ (where $h = 0$ represents plain convex and $h = 1$ represents strongly convex) achieves convergence rates $Y_t^{(w)} = O(t^{-h/(2-h)})$ and $Y_t^{(A)} = O(t^{-1/(2-h)})$ for diminishing step sizes $\eta_t = O(t^{-1/(2-h)})$. For this reason, when we study plain convex problems, we use diminishing step size sequence $O(t^{-1/2})$ and we experiment with different increasing sample size sequences to determine into what extent asynchronous SGD or Hogwild! is robust against delays. Since strongly convex problems have best convergence and therefore best robustness against delays, we expect a suitable increasing sample size sequence $O(i^p)$ for some $0 \leq p \leq 1$.

**For completeness, the leading term is also independent of $\|w_0 - w_*\|^2$ – it turns out that for $t \geq T_1 = \frac{\mu^2}{\alpha^2 N D} \|w_0 - w_*\|^2$ the higher order term that contains $\|w_0 - w_*\|^2$ is at most the leading term.

For non-convex (e.g., DNN) problems we generally use the averaged expected squared norm of the objective function gradients:

$$Y_t^{(\nabla)} = \frac{1}{t+1} \sum_{j=0}^t \mathbb{E}[\|\nabla F(w_j)\|^2].$$

This type of convergence rate analyses convergence to a stationary point, which is a candidate for any (good or bad) local minimum and does not exclude saddle-points. There may not even exist a global minimum (i.e., \mathcal{W}^* is empty) in that some entries in the weight vector w_t may tend to $\pm\infty$ – nevertheless, there may still exist a value $F_* = \sup\{F_{low} : F_{low} \leq F(w), \forall w \in \mathbb{R}^d\}$ which can be thought of as the value of the global minimum if we include limits to infinite points. In practice a diminishing step size sequence of $O(t^{-1/2})$ (as in the plain convex case) gives good results and this is what is used in our experiments.

D Experiments

In this section, we provide experiments to support our theoretical findings, i.e., the convergence of our proposed asynchronous SGD with strongly convex, plain convex and non-convex objective functions.

We introduce the settings and parameters used in the experiments in Section D.1. Section D.2 provides detailed experiments for asynchronous SGD with different types of objective functions (i.e., strongly convex, plain convex and non-convex objective functions), different types of step size schemes (i.e., constant and diminishing step size schemes), different types of sample size sequences (i.e., constant and increasing sample sizes) and different types of data sets at the clients' sides (i.e., unbiased and biased).

Our experiments are mainly conducted on LIBSVM^{††} and MNIST data sets.

D.1 Experiment settings

Simulation environment. For simulating the asynchronous SGD, we use multiple threads where each thread represents one compute node joining the training process. The experiments are conducted on Linux-64bit OS, with 16 cpu processors and 32Gb RAM.

Experimental setup. Equation (15) defines the plain convex logistic regression problem. The weight vector \bar{w} and bias value b of the logistic function can be learned by minimizing the log-likelihood function J :

$$J = - \sum_i^M [y_i \cdot \log(\sigma_i) + (1 - y_i) \cdot \log(1 - \sigma_i)], \text{ (plain convex)} \quad (15)$$

where M is the number of training samples (x_i, y_i) with $y_i \in \{0, 1\}$, $\sigma_i = \sigma(\bar{w}, b, x_i)$ and

$$\sigma(\bar{w}, b, x) = \frac{1}{1 + e^{-(\bar{w}^T x + b)}}$$

is the sigmoid function with as parameters the weight vector \bar{w} and bias value b . The goal is to learn a vector w^* which represents a pair $w = (\bar{w}, b)$ that minimizes J .

Function J can be changed into a strongly convex problem by adding a regularization parameter $\lambda > 0$:

$$\hat{J} = - \sum_i^M [y_i \cdot \log(\sigma_i) + (1 - y_i) \cdot \log(1 - \sigma_i)] + \frac{\lambda}{2} \|w\|^2, \text{ (strongly convex)},$$

where $w = (\bar{w}, b)$ is vector \bar{w} concatenated with bias b . For simulating non-convex problems, we choose a simple neural network (LeNet) [LeCun et al., 1998] for image classification.

The parameters used for our asynchronous SGD algorithm with strongly convex, plain convex and non-convex objective functions are described in Table 1.

^{††}<https://www.csie.ntu.edu.tw/~cjlin/libsvmtools/datasets/binary.html>

Table 1: Default asynchronous SGD training parameters

	Sample size sequence	# of compute nodes	Diminishing step size η_t	Reg. par. λ
Strongly convex	$s_i^\dagger = a \cdot i^c + b$	5	$\frac{\eta_0}{1+\beta t^{\frac{1}{2}}}$	$\frac{1}{M}$
Plain convex	$s_i = a \cdot i^c + b$	5	$\frac{\eta_0}{1+\beta t}$ or $\frac{\eta_0}{1+\beta\sqrt{t}}$	N/A
Non-convex	$s_i = a \cdot i^c + b$	5	$\frac{\eta_0}{1+\beta\sqrt{t}}$	N/A

\dagger This is the total sample size for the i -th communication round, i.e., $s_i = \sum_{c=1}^n s_{i,c}$ where $s_{i,c}$ is the sample size of client $c \in \{1, \dots, n\}$. By default $s_{i,c} = s_i/n$.

\ddagger The i -th round step size $\bar{\eta}_i$ is computed by substituting $t = \sum_{j=0}^{i-1} s_j$ into the diminishing step size formula.

For plain convex problems, we may use the diminishing step size schemes $\frac{\eta_0}{1+\beta \cdot t}$ or $\frac{\eta_0}{1+\beta \cdot \sqrt{t}}$, although our experiments in this paper focus on using $\frac{\eta_0}{1+\beta \cdot \sqrt{t}}$.

In our experiments we use parameter $\beta = 0.001$ for strongly convex problems and $\beta = 0.01$ for plain and non-convex problems. Parameter η_0 is the initial step size which we compute by performing a systematic grid search for β (i.e., we select the η_0 giving 'best' convergence).

When we talk about accuracy (in Table 2 and onward), we mean test accuracy defined as the the fraction of samples from a test data set that get accurately labeled by the classifier (as a result of training on a training data set by minimizing a corresponding objective function). Test error in Fig 9, 11, 12 means one minus the test accuracy.

Rather than test accuracy, we may measure convergence by plotting $F(w_t) - F(w^*)$, where F is the objective function (corresponding to J and \hat{J} for strongly and plain convex problems, and corresponding to LeNet for the non-convex problem of image classification). The value $F(w_t) - F(w^*)$ reflects how close the t -th iteration gets to the minimal objective function value. Here, we estimate the actual minimum w^* by using a single SGD with diminishing step sizes for a very large number of iterations .

D.2 Asynchronous SGD

We consider our asynchronous SGD with strongly convex, plain convex and non-convex objective functions for different settings, i.e., different step size schemes (constant and diminishing step size sequences), different sample size schemes (constant and increasing samples size sequences), and different type of the data sets (biased and unbiased data sets across compute nodes).

D.2.1 Asynchronous SGD with constant step size sequence and constant sample size sequence

The purpose of this experiment is to find the best constant sample size sequence we can use. We will use this in Section D.2.3 to compare constant step size and constant sample size sequences with diminishing step size sequences that use increasing sample sizes.

For simplicity, we set the total number of iterations at $K = 20,000$ for $n = 5$ compute nodes, and a constant step size $\eta = 0.0025$.

Table 2: The accuracy of asynchronous SGD with constant sample sizes

	Sample size	50	100	200	500	700	1000
	# of communication rounds	80	40	20	8	6	4
a9a	strongly convex	0.8418	0.8443	0.8386	0.8333	0.8298	0.7271
	plain convex	0.8409	0.8415	0.8417	0.8299	0.8346	0.7276
covtype.binary	strongly convex	0.8429	0.8402	0.8408	0.8360	0.8278	0.7827
	plain convex	0.8421	0.8438	0.8404	0.8381	0.8379	0.7287
mnist	non-convex	0.9450	0.9470	0.9180	0.8740	0.8700	0.7080

The results are in Table 2. We see that with constant sample size $s_i = 100$ or $s_i = 200$, we get the best accuracy for strongly convex, plain convex and non-convex cases, when compared to the other constant sample sizes. We notice that we can choose the small constant sample size $s_i = 50$ as well, because this also achieves good accuracy, however, this constant sample size requires the algorithm to run for (much) more communication rounds. In conclusion, we need to choose a suitable constant sample size, for example $s_i = 100$ or $s_i = 200$ to get a good accuracy and a decent number of communication rounds.

D.2.2 Asynchronous SGD with diminishing step size sequence and increasing sample size sequence

To study the behaviour of asynchronous SGD with different increasing sample size sequences, we conduct the following experiments for both $O(i)$ and $O(\frac{i}{\ln i})$ sequences. The purpose of this experiment is to show that these two sampling methods provide good accuracy.

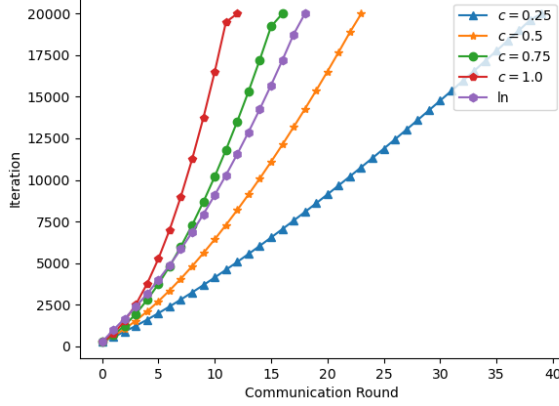
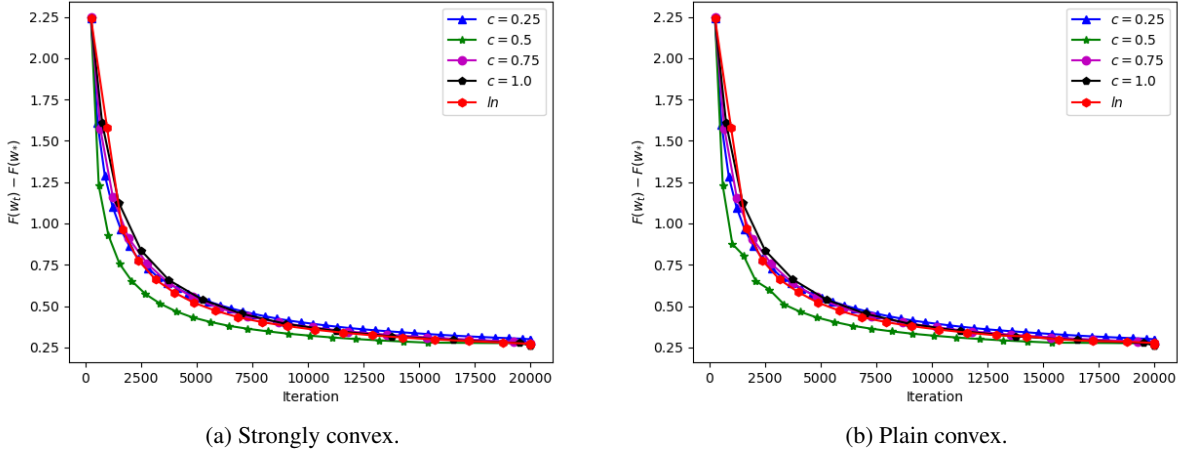


Figure 4: Number of communication rounds by sampling methods.



(a) Strongly convex.

(b) Plain convex.

Figure 5: Effect of sampling methods (a9a dataset).

Sampling method: In this paper, we choose two ways to increase the sample sizes from one communication round to the next. Let s_i be the number of iterations that the collection of all compute nodes runs in round i :

1. $O(i)$ method: $s_i = a \cdot i^c + b$ where $c \in [0, 1]$, $a, b \geq 0$.
2. $O(\frac{i}{\ln i})$ method: $s_i = a \cdot \frac{i}{\ln(i)} + b$ where $a, b \geq 0$.

For simplicity, we set $b = 0$, $a = 50$, and the total number of iterations at 20,000 for 5 compute nodes in Figure 4. We choose the diminishing step size sequence $\frac{\eta_0}{1+\beta \cdot t}$ for the strongly convex case and $\frac{\eta_0}{1+\beta \cdot \sqrt{t}}$ for the plain convex case, with initial step size $\eta_0 = 0.01$. From Figure 5 and Figure 6 we infer that $O(i)$ with $c = 1.0$ and $O(\frac{i}{\ln i})$ sample size sequences provide fewer communication rounds while maintaining a good accuracy, when compared to other settings. (For completeness, we verified that other increasing sample size sequences, such as exponential increase and cubic increase, are not good choices for our asynchronous SGD setting.)

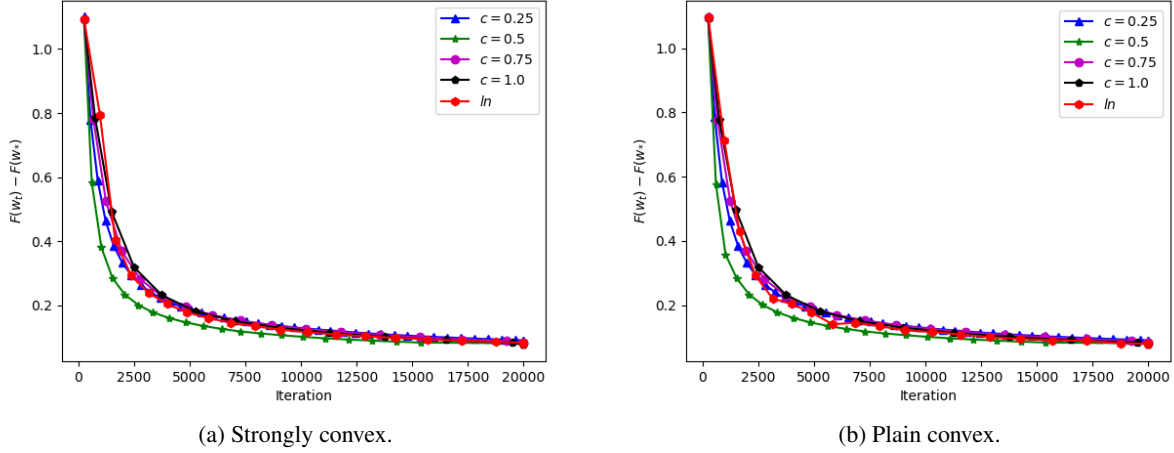


Figure 6: Effect of sampling methods (covtype-binary dataset).

D.2.3 Comparison asynchronous SGD with (constant step size, constant sample size) and (diminishing step size, increasing sample size).

In order to understand the behavior of the asynchronous SGD for different types of step sizes, we conduct the following experiments on strongly convex, plain convex and non-convex problems.

Diminishing step size scheme: We use the following two diminishing step size schemes:

1. Diminishing step size scheme over iterations (diminishing₁): Each compute node $c \in \{1, \dots, n\}$ uses η_t for $t = \sum_{a=1}^n (\sum_{j=0}^{i-1} s_{j,c} + h) = \sum_{j=0}^{i-1} s_j + n \cdot h$ where $i \geq 0$ denotes the current round, and $h \in \{0, \dots, s_{i,c} - 1\}$ is the current iteration which the compute node executes. In our experiments all compute nodes use the same sample sizes $s_{j,c} = s_j/n$.
2. Diminishing step size scheme over rounds (diminishing₂): Each client c uses a round step size $\bar{\eta}_i$ for all iterations in round i . The round step size $\bar{\eta}_i$ is equal to η_t for $t = \sum_{j=0}^{i-1} s_j$.

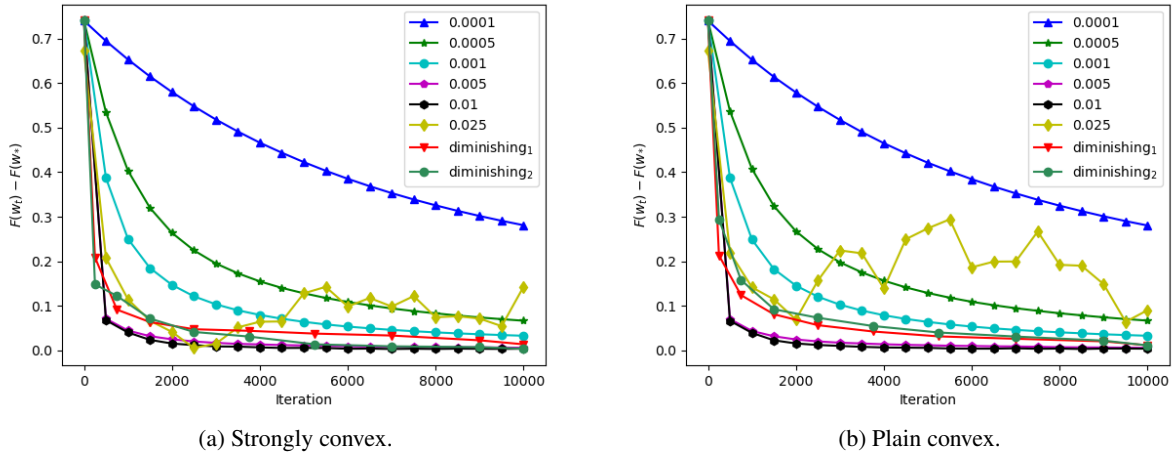


Figure 7: Convergence rate with different step sizes (phishing dataset)

The detailed setup of this experiment is described in Table 1. In terms of diminishing step size, the experiment will start with the initial step size $\eta_0 = 0.1$. The experiment uses a linear increasing sample size sequence from round to round.

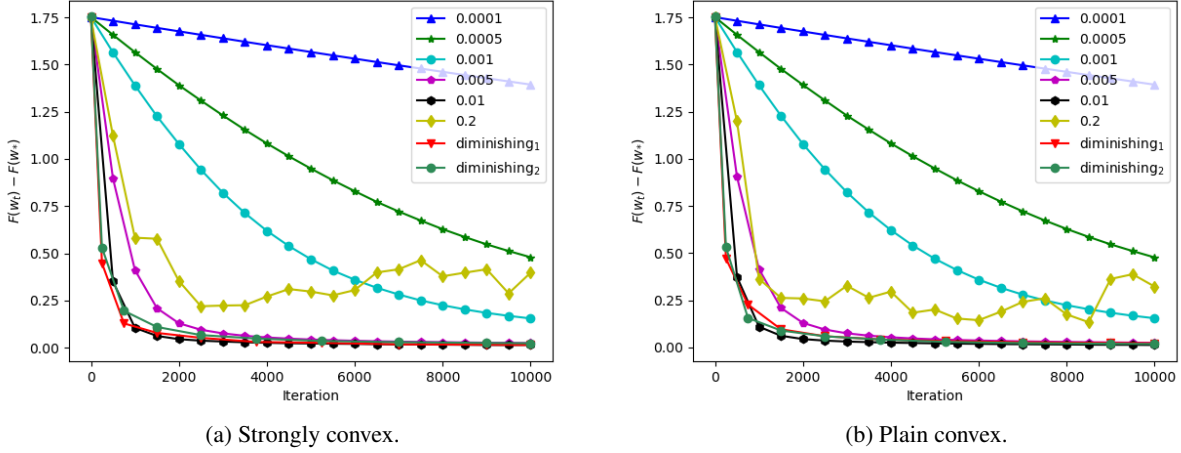


Figure 8: Convergence rate with different step sizes (ijcnn1 dataset)

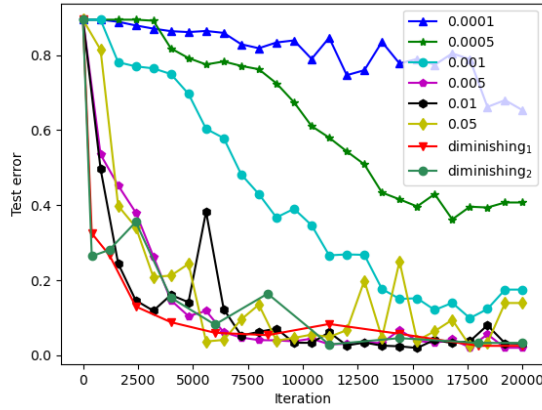


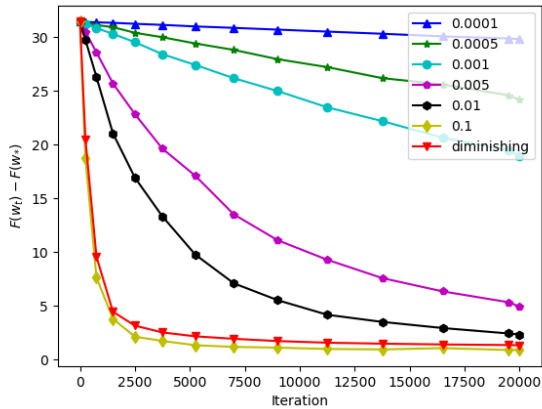
Figure 9: Asynchronous SGD in non-convex (MNIST dataset)

Strongly convex case: Figure 7a and Figure 8a show that our proposed asynchronous SGD with diminishing step sizes and increasing sample size sequence achieves the same or better accuracy when compared to asynchronous SGD with constant step sizes and constant sample sizes. The figures depict strongly convex problems with diminishing step size scheme $\eta_t = \frac{\eta_0}{1+\beta \cdot t}$ for an initial step size $\eta_0 = 0.1$ with a linearly increasing sample size sequence $s_i = a \cdot i^c + b$, where $c = 1$ and $a, b \geq 0$; diminishing₁ uses a more fine tuned η_t locally at the clients and diminishing₂ uses the transformation to round step sizes $\bar{\eta}_i$. The number of communication rounds, see Figure 7 as example, for constant step and sample sizes is 20 rounds, while the diminishing step size with increasing sample size setting only needs 9 communication rounds.

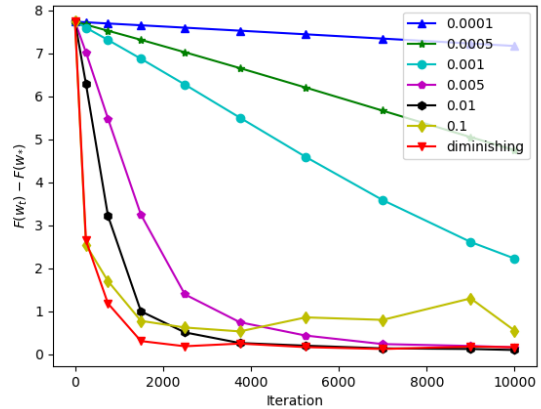
Plain convex case: We repeat the above experiments for plain convex problems. Figure 7b and Figure 8b illustrate the same results for the diminishing step size sequence $\eta_t = \frac{\eta_0}{1+\beta \cdot \sqrt{t}}$, $\eta_0 = 0.1$ with increase sample size sequence $s_i = a \cdot i^c + b$, where $c = 1$ and $a, b \geq 0$.

Non-convex case: We run the experiment with the MNIST data set using the LeNet-5 model. We choose a diminishing step size sequence by decreasing the step size by $\eta_t = \frac{\eta_0}{1+\beta \cdot \sqrt{t}}$, $\eta_0 = 0.1$ and use sample size sequence $s_i = a \cdot i^c + b$, where $c = 1$ and $a, b \geq 0$. The detailed result of this experiment is illustrated in Figure 9.

In addition, for the strongly convex problems we extend our experiments to constant step size sequences, while still linearly increase the sample sizes $s_i = a \cdot i^c + b$, where $c = 1$ and $a, b \geq 0$, from round to round. The difference



(a) Strongly convex (real-sim dataset).



(b) Strongly convex (w8a dataset).

Figure 10: Asynchronous SGD (linearly increase sampling) with constant and diminishing step sizes.

between using a constant step size sequence plus increasing sample size sequence and diminishing step size sequence (starting at $\eta_0 = 0.01$) plus increasing sample size sequence can be found in Figure 10. Overall, our asynchronous SGD with diminishing step sizes gains good accuracy, which can only be achieved by fine tuning constant step sizes to $\eta = 0.01$ and $\eta = 0.005$ for the two data sets respectively.

In conclusion, our proposed asynchronous SGD with diminishing step size sequences and increasing sample size sequences works effectively for strongly convex, plain convex and non-convex problems because it can achieve the best accuracy when compared to other constant step size sequences while requiring fewer communication rounds.

D.2.4 Asynchronous SGD with biased and unbiased data sets

To study the behaviour of our proposed framework towards biased and unbiased data sets, we run a simple experiment with in total 10,000 iterations for 2 compute nodes, where each compute node has its own data set. The goal of this experiment is to find out whether our proposed asynchronous SGD can work well with biased data sets. Specifically, the first compute node will run for a data set which contains only digit 0 while the second client runs for a data set with only digit 1. Moreover, we choose the initial step size $\eta_0 = 0.01$ and a linearly increasing sample size sequence $s_i = a \cdot i^c + b$, where $c = 1$ and $a, b \geq 0$ for strongly convex and plain convex problems. For simplicity, we choose diminishing round step size sequence corresponding to $\frac{\eta_0}{1+\beta \cdot t}$ for the strongly convex problem and $\frac{\eta_0}{1+\beta \cdot \sqrt{t}}$ for the plain convex problem.

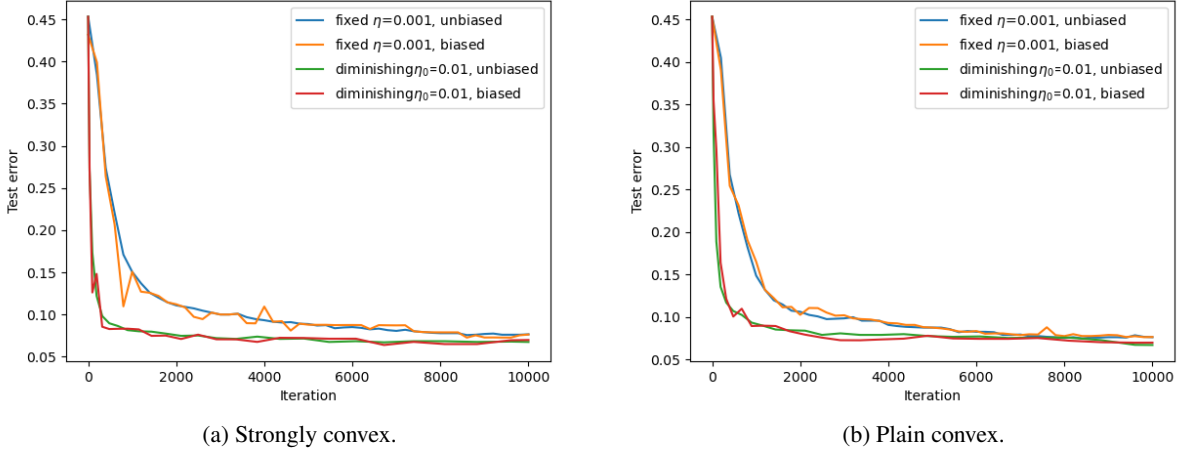


Figure 11: Asynchronous SGD with biased and unbiased dataset (MNIST subsets)

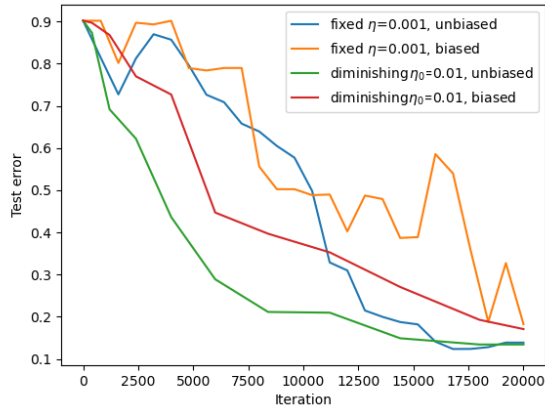


Figure 12: Asynchronous SGD with biased and unbiased dataset (MNIST dataset)

As can be seen from Figure 11, generally, there is no significant difference when compute nodes run for biased or unbiased local data sets. This means that our proposed SGD framework can tolerate the issue of biased data sets, which is common in reality. Turning to the non-convex problem, we extend this experiment to the MNIST dataset, where the local data set of each compute node is separately biased, i.e., each of (the 5) compute nodes just has a separate subset of 2 classes of MNIST digits (hence, covering all $5 \cdot 2$ digits). The experiment uses the initial step size $\eta_0 = 0.01$ with diminishing round step size sequence corresponding to $\frac{\eta_0}{1+\beta \cdot \sqrt{t}}$. Figure 12 shows that while the accuracy might fluctuate during the training process, our asynchronous SGD still achieves good accuracy in general.

In conclusion, our asynchronous SGD framework works well under biased data sets, i.e., this framework can tolerate the effect of biased data sets, which is quite common in reality.

D.2.5 Asynchronous SGD with different number of compute nodes

We want to understand how varying the number n of compute nodes while fixing other parameters, such as the total number of iterations $K = 20,000$ and diminishing step size sequence, affects the accuracy. The goal of this experiment is to show that the number of clients n can not be arbitrary large due to the restriction from the delay function τ .

To make the analysis simple, we consider asynchronous SGD with $d = 1$ (i.e., each compute node is allowed to run faster than the central server for at most 1 communication round) and unbiased data sets. Moreover, we choose a linearly

increasing sample size sequence $s_i = a \cdot i^c + b$, where $c = 1$ and $a = 50, b = 0$ for strongly convex and plain convex problems. The experiment uses an initial step size $\eta_0 = 0.01$ with diminishing round step size sequence corresponding to $\frac{\eta_0}{1+\beta \cdot t}$ and $\frac{\eta_0}{1+\beta \cdot \sqrt{t}}$ for strongly convex and plain convex problems respectively.

Table 3: Test accuracy of asynchronous SGD with different number of compute nodes, strongly convex (phishing dataset)

# of compute nodes	Accuracy (%)	Duration (in second)
1	0.9355	338
2	0.9354	169
5	0.9297	57
10	0.9202	24
15	0.9134	17
20	0.9069	16
30	0.9005	16

Table 4: Test accuracy of asynchronous SGD with different number of compute nodes, plain convex (phishing dataset)

# of compute nodes	Accuracy (%)	Duration (in second)
1	0.9341	324
2	0.9303	164
5	0.9258	53
10	0.9247	26
15	0.9215	16
20	0.9135	15
30	0.9047	15

As can be seen from Table 3 and Table 4, when we increase the number of compute nodes n , the training duration decreases gradually. Specifically, when $n = 1$ (SGD with single machine) we achieve the best accuracy, compared to other settings. When $n = 2$ or $n = 5$, we get the same accuracy, compared to a single SGD setting while reducing the training time significantly. However, if we continue to increase n to a large number, for example $n = 30$, then the accuracy has the trend to decrease and training duration starts to reach a lower limit.

We first note that the lower accuracy is an artifact of our simulation: We split the training data set of size M among each of the compute nodes (according to some random process). This means that each compute node uses its own M/n -sized local data set. The larger n , the smaller the local data sets, and as a result the local data sets are less representative of distribution \mathcal{D} (the uniform distribution over the original M -sized training data set). In other words, the local distributions \mathcal{D}_c start looking less and less like one another. This implies a shift from unbiased local data sets to biased local data sets for increasing n . This leads to a slight degradation in accuracy (see previous Section D.2.4). If local data sets remain very large sample sets of the original training data, then we will keep on seeing the accuracy corresponding to unbiased local data sets (and this is what one would expect in practice).

Next we note that we are more likely to have a slow compute node among n nodes if n is large. The slowest compute node out of n nodes is expected to be slower for increasing n . This means that other compute nodes will need to start waiting for this slowest compute node (see the while $\tau(t_{glob}) \leq t_{delay}$ loop in MAINCOMPUTENODE which waits for the server to transmit a broadcast message once the slowest compute node has finished its round and communicated its update to the server). So, a reduction in execution time due to parallelism among a larger number n of compute nodes will have less of an effect. For increasing n , the execution time (duration) will reach a lower limit.

For larger n , the central server will process/aggregate a larger number of local updates – nevertheless, since sample sizes increase from round to round, this should not become a bottleneck in later rounds (implying that compute nodes will not need to wait for the server finishing its computations/aggregations).

In our simulations we see that a lower limit for the duration is reached for 15 compute nodes. We also see the same result for the experiment with non-convex problem, which can be seen in Table 5. This experiment uses the initial step size $\eta_0 = 0.01$ with diminishing round step size sequence corresponding to $\frac{\eta_0}{1+\beta \cdot \sqrt{t}}$.

As a final remark, if local data happens to be stored at many nodes in for example a data center, then our algorithm still scales to that setting: The compute nodes are used to bring computation to the data. They also compute in parallel but this will only reduce the full execution time/duration to a lower limit (after which parallelism will not further benefit a

shorter full execution time). The increasing sample size sequence will still reduce communication with respect to a constant sample size sequence or fixed sized mini-batch SGD.

Table 5: Test accuracy of asynchronous SGD with different number of compute nodes, non-convex (MNIST dataset)

# of compute nodes	Accuracy (%)	Duration (in second)
1	0.9838	513
2	0.9815	403
5	0.9797	117
10	0.9177	77
15	0.8809	75

D.2.6 Asynchronous SGD with different number of iterations

We now want to understand how varying the total number of iterations $K = 20,000$ while fixing other parameters, such as the number n of compute nodes and diminishing step size sequence, affects the accuracy. The goal of this experiment is to show that from some point onward it does not help to increase the number of iterations. This is because the test accuracy is measured with respect to a certain (test) data set of samples from distribution \mathcal{D} for which the fraction of correct output labels is computed. Such a fixed test data set introduces an approximation error with respect to the training data set; the training accuracy which is minimized by minimizing the objective function is different from the test accuracy. Therefore, it does not help to attempt to converge closer to the global minimum than the size of the approximation error. Hence, going beyond a certain number of iterations will not reduce the estimated objective function (by using the test data set) any further.

To make the analysis simple, we consider asynchronous SGD with $d = 1$ (i.e., each compute node is allowed to run faster than the central server for at most 1 communication round) and unbiased data sets. Moreover, we choose a linearly increasing sample size sequence $s_i = a \cdot i^c + b$, where $c = 1$ and $a = 50, b = 0$ for strongly convex and plain convex problems. The experiment uses an initial step size $\eta_0 = 0.01$ with diminishing round step size sequence corresponding to $\frac{\eta_0}{1+\beta \cdot t}$ and $\frac{\eta_0}{1+\beta \cdot \sqrt{t}}$ for strongly convex and plain convex problems respectively. For simplicity, our simulation is based on 5 compute nodes (together with the central aggregation server).

Our observation from Table 6,7,8 is when the number of iterations is 50,000, we gain the highest accuracy. In addition, if we continue to increase the number of iterations, the accuracy keeps nearly unchanged, i.e, a larger number of iterations does not improve accuracy any further.

Table 6: Test accuracy of asynchronous SGD with different number of iterations, strongly convex (phishing dataset)

# of iterations	Accuracy (%)
1,000	0.9062
2,000	0.9139
5,000	0.9211
10,000	0.9231
20,000	0.9257
50,000	0.9323
100,000	0.9301

Table 7: Test accuracy of asynchronous SGD with different number of iterations, plain convex (phishing dataset)

# of iterations	Accuracy (%)
1,000	0.9003
2,000	0.9108
5,000	0.9149
10,000	0.9241
20,000	0.9264
50,000	0.9361
100,000	0.9343

Table 8: Test accuracy of asynchronous SGD with different number of iterations, non-convex (MNIST dataset)

# of iterations	Accuracy (%)
1,000	0.4064
2,000	0.7613
5,000	0.9378
10,000	0.9642
20,000	0.9798
50,000	0.9868
100,000	0.9892